

ResearchOnline@JCU

This file is part of the following reference:

Fay, C. (2014) *Modeling, describing, measuring and interpreting porphyroblast inclusion trails to understand inter-relationships between deformation, metamorphism and tectonism*. PhD thesis, James Cook University.

Access to this file is available from:

<http://researchonline.jcu.edu.au/39976/>

The author has certified to JCU that they have made a reasonable effort to gain permission and acknowledge the owner of any third party copyright material included in this document. If you believe that this is not the case, please contact

*ResearchOnline@jcu.edu.au and quote
<http://researchonline.jcu.edu.au/39976/>*

**MODELING, DESCRIBING, MEASURING AND INTERPRETING
PORPHYROBLAST INCLUSION TRAILS TO UNDERSTAND INTER-
RELATIONSHIPS BETWEEN DEFORMATION, METAMORPHISM
AND TECTONISM**

Volume I

(Text)

Thesis submitted by

C.Fay, Bsc Université Lyon I,

Msc ENS Lyon – Université Nice Sophia Antipolis, France.

In November 2014

For the degree of Doctor of Philosophy

in the College of Science, Technology and Engineering

James Cook University

STATEMENT ON THE CONTRIBUTION OF OTHERS

The following Phd research project was conducted under the supervision and close intellectual collaboration of Pr. T.H. Bell.

The first chapter presented in this thesis was published in *Geology* with the important help of Dr. B.E. Hobbs and Pr. T.H. Bell who co-authored in this paper. The ratio of contribution for this publication is about 50% Fay and 25% for both Hobbs and Bell.

The intellectual and editorial contributions for the remaining chapters are shared between Bell and Fay with respectively:

- 70% Fay, 30 % Bell for chapter II
- 45% Fay, 55% Bell for chapter III
- 90% Fay, 10% Bell for chapter IV

Most of the samples used in chapter II to IV were collected by A. Ali and I. V. Sanislav.

Funding for the acquisition of modeling software was provided by an ARC grant attributed to T.H. Bell. Analysis expenses were supported by JCU GRS grants awarded to C.Fay.

ACKNOWLEDGEMENTS

I must start by stating that I could never be too grateful to Tim Bell for his constant support through the years. Thank you Tim, for your tremendous mentoring and intellectual emulation. Thank you for this great scientific journey.

I want to thank dearly Dr. B.E. Hobbs for his sharp-mind and great collaboration; Dr. M. J .Rubenach for his passion of metamorphic petrology and his constant enthusiasm about sharing his knowledge in this field.

Many thanks to all the SAMRI international crew, Afroz Shah, Jyo-tyndra Sapkota, Ashgar Ali, Ahmed and Hui Cao for providing such a great and fun working atmosphere. A special thanks to Mark Munroe, Ioan Sanislav, and “gros” Raph (bises pour tout mec) for their friendship and passion of geology.

Thank you to Zuzu, Rodrigues, Lucas, Sammy, Marc, Condo, David, Rebecca, Craig, Elkie and Bree, and all the talented musicians that are found only in the tropics. I wouldn't have been able to make Townsville home if I you were not around and cranking crazy tropical music jams.

Thank you to Morgane Moreau and Jean Baptiste Raina for your truthful friendships. Special thanks to Mitch Goodwin for always taking things to another level.

Incredible thank you to my parents, Claire and Eric and my sisters Madeleine and Priscille for their material and moral support.

To my genius and best wife in the world Michelle Hall, that buys me cheese when I am stressed. Thank you for sharing your life with me, and dancing with me in the kitchen.

THESIS ABSTRACT

The main objectives of the research presented in this PHD thesis are:

- to demonstrate numerically the relevance of using microstructures encapsulated within porphyroblasts as a quantitative proxy for unravelling lengthy orogenic deformation history;
- applying this quantitative measurements of foliation intersection/inflexion axis (FIAs) method to deciphering the sequence of main shortening directions responsible for most of the deformation features observed in fold interference patterns and the arcuate shape of orogens using the example of the Adelaide Geosyncline (South Australia);
- to describe with great precision the sequence of deformation and metamorphic events and their inter-relationships during one single FIA event affecting the study area;
- to understand the long-lasting stable metamorphic conditions of mid-crustal rocks displaying multiple generations of synchronous staurolite and andalusite using a combination of thermo-dynamic modelling coupled with microstructural analysis.

The first part is based on the data on foliation intersection/inflexion axes preserved in porphyroblasts (FIAs) and show that no porphyroblast rotation occurs during ductile deformation relative to spatial coordinates. This contrasts with 99% of investigations of “rigid” objects in non-coaxially deforming media where the objects rotate. When anastomosing shear zone formation around relatively strong objects in a weaker matrix is modelled, no “porphyroblast” rotation occurs. Formation of these anastomosing zones controls the development of this phenomenon, labelled “gyrostatic”. If such zones are absent, porphyroblasts rotate. In weak materials the gyrostatic situation arises because the superposition of simple shearing deformation normal to initial coaxial shortening results in only small rotations of principal axes of stress. Since shear zones are controlled by the orientations of principal axes of stress, initial anastomosing zones retain their orientations and positions during subsequent non-coaxial deformation. The porphyroblast is isolated from the embedding non-coaxially deforming material and material close to the porphyroblast continues to deform

coaxially; no local rotation occurs. This has major significance since porphyroblasts can be routinely used to access lengthy tectonic histories destroyed in the matrix by reactivation. In particular, changes in relative directions of bulk shortening, associated with orogenesis, can now be determined within ancient orogens.

In the second part of the thesis, porphyroblast microstructures in rocks from a narrow portion of the sigmoidal-shaped Adelaide geosyncline indicate that the Delamerian Orogeny was a product of five changes in the direction of bulk shortening. The progression from NNW-SSE to WSW-ENE to SSW-NNE to WNW-ESE to NNE-SSW directed bulk shortening, resulted from shifts in the direction of relative plate motion as orogenesis progressed between 522 and 478 Ma. These directions were determined from a succession of 5 FIAs (Foliation Intersection/Inflection Axes preserved within porphyroblasts). The overprinting relationships between the multiple generations of regional folds that developed were resolved using the timing criteria provided by this FIA succession. The S-shape of the orocline has been interpreted as a fold and thrust belt product of either oblique convergence or the development of asymmetric syntaxis zones but this is not the case. Rather the orocline resulted the overprinting of a succession of near orthogonal plan view changes in the direction of convergence. This reflects much of the geodynamic evolution of the Eastern Australian portion of the Gondwana margin during its early Paleozoic history.

In the third part of the thesis, excellent inclusion trails in a staurolite and andalusite-bearing sample preserve 3 main phases of growth of both phases during the early stages of 3 deformation events. Subtle extra periods of growth of both phases occur, being most obvious for andalusite porphyroblasts, which commonly occur as clusters of large crystals that vary from several to tens of degrees in orientation and can encapsulate staurolite grown in an earlier or the same deformation event. All foliations defined by all inclusion trails intersect in a FIA (a foliation intersection axis preserved within porphyroblasts) trending at 25° indicating no change in the direction of horizontal components of bulk shortening while the porphyroblasts grew. Well-preserved microstructural relationships between successive foliations within porphyroblasts allow a detailed analysis of the approaches to inclusion trail description and interpretation that have resulted from 25 years of quantitative FIA based studies. Spiral-shaped inclusion trails in most porphyroblast clusters contain portions of

millipede geometries. The latter clinch the dominant role of bulk shortening in porphyroblast growth even in an environment that is overall non coaxial and which results in the same asymmetry later on in each deformation event. Any role for porphyroblast rotation is strongly refuted by differing stages in the development of these bulk-shortening geometries preserved within staurolite and the andalusite that immediately enclosed them as does such variation in adjacent clusters. They strongly suggest that discrepancy in the orientation of inclusion trails in porphyroblast cores is a function of the early effects of bulk shortening driving porphyroblast growth and cannot be used to imply later porphyroblast rotation. Staurolite and andalusite have grown slightly before, after and synchronously, without reacting with each other, during the early stages of 3 separate deformations. This strongly supports microstructural and more recent metamorphic data that the early stages of bulk shortening start porphyroblast growth; it also indicates that the commencement of the development of a differentiated foliation in the vicinity of a porphyroblast will always stop growth.

In the four part of this thesis, it is revealed that the southern portion of the Adelaide fold belt contains a large region where synchronous to interleaved growth of staurolite and andalusite porphyroblasts has occurred. The truncation and continuity of inclusion trails versus matrix foliations reveal multiple periods of growth of staurolite and andalusite in many samples. The measurement of FIAs (foliation intersection axes preserved within porphyroblasts) revealed a succession of 5 changes in the bulk shortening direction during orogenesis from initially NNW-SSE when the first FIA (I), trending at 75° , formed in garnet. FIAs II through V are present in garnet, staurolite and andalusite. Indeed, staurolite and andalusite grew in the same sample during the development of at least one of FIAs II, III, IV and V. Pseudosections show a remarkably narrow range of PT conditions where this is possible and define a very confined location in PT space where these rocks developed at least 10 foliations over the ~ 30 million years that FIAs II through V developed. Garnet growth occurred early in some samples, but not in others with very similar bulk chemistry, where staurolite and andalusite grew in the same FIA event. This behaviour resulted from slight changes in Mn content and allowed a very tightly constrained PT path to be defined on pseudosections in combination with the minerals that formed early and late in some multi FIA samples. These low-pressure high-temperature rocks remained at the same orogenic level throughout most of the very lengthy deformation history of the Delamerian orogenic cycle once staurolite and andalusite began to grow. They ceased to

grow at the commencement of exhumation when retrogressive chlorite growth began in many samples when shortening was directed once again NNW-SSE.

Keywords: Porphyroblast continuum modeling, millipede microstructures, FIAs, Kanmantoo group, Adelaide geo-syncline, Gondwana , S-shape Orocline, spiral trails from millipeding, multiple phases of porphyroblast growth, synchronous staurolite and andalusite growth, PT stability during orogenesis.

CONTENT OF VOLUME I

STATEMENT ON THE CONTRIBUTION OF OTHERS.....	<i>i</i>
ACKNOWLEDGMENT.....	<i>ii</i>
THESIS ABSTRACT.....	<i>iii-vi</i>
TABLE OF CONTENTS.....	<i>vii</i>
INTRODUCTION AND THESIS OUTLINE.....	<i>p1-8</i>
-CHAPTER I-.....	<i>p9-26</i>
<i>Porphyroblast rotation versus non-rotation: conflict resolution!</i>	
-CHAPTER II-.....	<i>p27-55</i>
<i>Polyphase tectonism and orocline development revealed by spatial shifts in deformation partitioning</i>	
-CHAPTER III-.....	<i>p56-89</i>
<i>Inclusion trail analysis techniques, multiply interleaved growth of staurolite and andalusite, and shifting of reaction vs deformation with time</i>	
-CHAPTER IV-.....	<i>p90-111</i>
<i>The significance for metamorphism, orogenesis and PT paths of ~40 million years of multiple phases of deformation and effectively synchronous staurolite-andalusite growth</i>	
GENERAL CONCLUSIONS.....	<i>p112-115</i>

INTRODUCTION AND THESIS OUTLINE

This thesis uses multiple approaches to understand the significance of foliations preserved as inclusion trails in porphyroblast minerals. One approach involved the experimental testing of theoretical and numerical models that possibly provided an analytical solution for the non-rotation of large rigid object in continuum mechanics. Prior to that study most analyses of the kinematics of rigid objects embedded in deforming rocks suggested that they rotated in a non-coaxial deformation environment (e.g., Jeffery, 1922; Ghosh and Ramberg, 1976; Ferguson, 1979; Ildefonse et al., 1992; Jezek, 1994; Masuda et al., 1995; Pennacchioni et al., 2000; Marques and Coelho, 2001; ten Grotenhuis et al., 2002; Ghosh et al., 2003; Jiang and Williams, 2004). However, these studies did not know about or ignored the role of anastomosing zones of progressive shearing and shortening in the formation of millipede geometries (Bell, 1981). It was these that appeared geometrically and conceptually to produce non-rotation in rocks during ductile deformation provided the porphyroblasts that overgrew them did not internally strain (Bell, 1985).

Another approach involved utilizing data on fold axial planes that can be measured from regional maps such as that used by Bell & Sanislav (2011). The Adelaide geosyncline contains two main stratigraphic units, the Proterozoic (800-600 Ma) Adelaidean Formation which is conformably overlain by the early-Cambrian flysch-like sequence of the Kanmantoo Group (Daily & Milnes, 1973; Von der Borch, 1980). Deformed during the Delamerian orogeny, the Adelaide geosyncline appears relatively simple on the large scale. Gently doubly-plunging folds with a steeply dipping axial plane slaty cleavage lie parallel to much of its length (e.g., Bell, 1978). Both rotate from N-S trends/strikes east of Adelaide to W-E ones to the south and north around two oroclinal arcs to form a very large scale S-shaped orogen and three

conflicting models have been suggested for how this shape developed (Coward, 1976; Clarke & Powell, 1989; Marshak & Flöttmann, 1996). However, locally, where the rocks become schistose, the steeply-dipping, axial plane cleavage to these orogen parallel folds is a differentiated crenulation cleavage. A much-studied example of this is that lying axial plane to the Strathalbyn anticline/Macclesfield syncline fold couplet (Offler & Fleming, 1968). A solution to the transition from slaty to differentiated crenulation cleavage was provided by Adshead-Bell & Bell (1999) using well preserved inclusion trails in staurolite and andalusite porphyroblasts. The statistical approach to fold axial planes trends (Bell & Sanislav, 2011) suggests a history of multiple deformation with several distinct peaks in the distribution along the orogen. Combined with local fold overprinting the potential for resolving part of the succession of deformations was obvious, but how did one correlate from arm to arm across the two oroclinal arcs.

This led to the approach that FIAs (foliation inflection/intersection lineations preserved in porphyroblasts) provide for understanding the deformation history of an oroclinal orogen (e.g., Bell & Mares, 1999). Access to porphyroblasts was not obvious on all of three arms of the orocline. However, Bell & Sanislav (2011) had suggested that hotter rocks where porphyroblasts grow may show up most or even all the history that large portions of an orogen had undergone. They argued that the heat weakens these rocks relative to those surrounding them plus increases the competency contrast between the large porphyroblast and the fine-grained matrix, which preferentially will partition even very weak deformation events against their rims. Furthermore, foliations preserved as inclusion trails in porphyroblastic rocks from the South Eastern part of the belt (Petrel Cove, Steinhardt, 1989; Southern Mount Lofty range, Adshead-Bell & Bell, 1999) suggesting a more complex tectonic history had been documented. Some FIAs

had been measured within these porphyroblasts prior to this study (none had been published) but no chronology had been established for a well-sampled region. Thus it appeared from both the initial experimental modelling of porphyroblast behaviour and the statistical distribution of regional fold axial planes that FIAs might provide a means of resolving the history of structural development.

The success of the above approach described below and the complex growth histories that were revealed by excellent inclusion trails in both staurolite and andalusite in several samples led to the detailed examination of how the inclusion trails progressively developed in one sample about a single FIA. The techniques for doing this have been described in detail and the revelations about how many spiral-shaped inclusion trails may form were documented, particularly the early role of near coaxial shortening during the early stages of each phase of porphyroblast growth.

The above approach led to that of constructing pseudosections using Thermocalc for several samples in which both staurolite and andalusite growth had occurred during at least one FIA event. Samples were selected where this had occurred for most of the FIAs in the succession that had been documented previously in order to see how interleaved to synchronous growth of these 2 phases was possible. This resulted in the generation of PT information that was tightly controlled in PT space on where the rocks were located and how they were behaving during a lengthy period of orogenesis.

Consequently, this thesis consists of four chapters. Each is written to be suitable for publication in international journals. The chapters are arranged to avoid repetition. Volume I contains the text and references. The figures are all contained in Volume II so that they can be examined with ease while reading the text.

Chapter I uses numerical modelling to investigate the behaviour of rigid objects during ductile deformation. 2D mechanical and thermo-mechanical finite element

models were computed to understand the role of deformation paths in the localization of deformation in the rotation or non-rotation of porphyroblast in non-coaxially deforming rocks. Prior to this approach it was widely accepted from theoretical, analogue and numerical investigations that non-rotation of large rigid object was not possible in continuum mechanics. This did not accord with the incredible consistency of data on the orientation of foliation intersection/inflection axes preserved within porphyroblast (FIAs) that has been published over two decades. We set out to reproduce the microstructural environment in which porphyroblasts actually grow as Bell has argued since 1981 that it was the key to why porphyroblasts did not rotate. When that was achieved, the porphyroblasts ceased to rotate even when deformation was continued in a purely non coaxial environment with no component of a bulk shortening.

Chapter II attempts to resolve the deformation sequence that led to the overall oroclinal S-shape of the Adelaide Geosyncline and the fold interference patterns within it. Correlating the deformation events responsible for folds at orogen scale is generally ambiguous, especially around oroclinal arcs, resulting in several competing geodynamic models. Data that can be measured from geological and geophysical maps along the whole orogen are used to determine the statistical distributions of fold axial plane trends. Foliation inflection/intersection axes preserved within porphyroblasts (FIAs) are measured from rocks in a relatively small but hot portion of the orogen that has been affected by regional metamorphism and many deformations. They provide a succession of changes in bulk shortening directions that can be compared with the statistical distribution of axial planes and fold overprinting criteria from along the orogen. The experimental results of Chapter 1, that porphyroblasts will not rotate if they nucleate and grow in zones being coaxially strained at a similar scale when deformation commences, can be tested. If this approach resolves the history of development of the

large-scale S-shaped orocline defined by the Adelaide Geosyncline, it should be applicable to any orocline that locally contains porphyroblastic rocks.

Chapter III is based on one sample from the Western part of the Kanmantoo group (South Australia) that provides considerable insight into the inter-relationships between deformation and metamorphism. This sample contains excellent inclusion trails that microstructurally suggest multiple phases of growth of both staurolite and andalusite porphyroblasts have occurred about the same FIA trend. Detailed analysis of these porphyroblast inclusion trails reveals the development of partial millipede geometries and histories of progressive bulk shortening within what superficially appear to be non-coaxial spiral inclusion geometries. Other microstructural/metamorphic relationships are revealed that confirm and advance microstructural understanding gained from previous studies of the development of inclusion trails within porphyroblasts.

Chapter IV uses the metamorphic history revealed by the Kanmantoo group FIAs in 7 samples with similar bulk compositions to examine the possibility of multiple growth of a given porphyroblastic phase. Phase diagram modelling of samples with where synchronous growth of staurolite and andalusite has occurred provides tight constraints on the temperature and pressure of the rocks when they experienced a given FIA event. The resulting lengthy history suggests very lengthy residence times for rocks within the metamorphosing cores of an orogen versus that leading to their expulsion towards the surface.

REFERENCES

- Adshead-Bell, N.S. & Bell, T.H., 1999. The progressive development of a macroscopic upright fold pair during five near orthogonal foliation production events: complex microstructures versus a simple macrostructure. *Tectonophysics*, **306**, 121-147.
- Bell, T.H., 1981. Foliation development: the contribution, geometry and significance of progressive bulk inhomogeneous shortening. *Tectonophysics*, **75**, 273-296.
- Bell, T.H., 1985. Deformation partitioning and porphyroblast rotation in metamorphic rocks: A radical reinterpretation. *Journal of Metamorphic Geology*, **3**, 109-118.
- Bell, T.H., Sapkota, J., 2012. Episodic gravitational collapse and migration of the mountain chain during orogenic roll-on in the Himalayas. *Journal of Metamorphic Geology* **30**, 651-666.
- Clarke, G. L. & Powell, R. 1989. Basement/cover interaction in the Adelaide Foldbelt, South Australia: the development of an arcuate foldbelt. *Tectonophysics* , **158**, 209-226.
- Coward, M. P. 1976. Large scale Palaeozoic shear zone in Australia and present extension to the Antarctic Ridge. *Nature* , **259**, 648-649.
- Daily, B. & Milnes, A. R. 1973. Stratigraphy, structure and metamorphism of the Kanmantoo Group (Cambrian) in its type section east of Tungkilla Beach, South Australia. *Trans. R. Soc. S.Aust.* , **97**, 213-242.
- Ferguson, C.C., 1979. Rotations of elongate rigid particles in slow non-Newtonian flows. *Tectonophysics*, **60**, 247-262.
- Ghosh, S.K., and Ramberg, H., 1976. Reorientation of inclusions by combination of pure shear and simple shear. *Tectonophysics*, **34**, 1-70.

- Ghosh, S.K., Sen, G., and Sengupta, S., 2003. Rotation of long tectonic clasts in transpressional shear zones: *Journal of Structural Geology*, v. 25, p. 1083-1096.
- Hayward, N., 1990. Determination of early fold axis orientations in multiply deformed rocks using porphyroblast inclusion trails. *Tectonophysics*, **179**, 353–369.
- Ildefonse, B., Sokoutis, D., and Mancktelow, N.S., 1992. Mechanical interactions between rigid particles in a deforming ductile matrix: analog experiments in simple shear-flow. *Journal of Structural Geology*, **14**, 1253-1266.
- Jeffery, G.B., 1922. The motion of ellipsoidal particles immersed in a viscous fluid. *Proceedings of the Royal Society of London*, **A102**, 161-179.
- Jezeq, J., 1994. Software for modelling the motion of rigid triaxial ellipsoidal particles in viscous flow. *Computers and Geosciences*, **20**, 409-424.
- Jiang, D., and Williams, P. F., 2004. Reference frame, angular momentum, and porphyroblast: *Journal of Structural Geology*, **26**, 2211-2224.
- Marques, F.O., and Coelho, S., 2001. Rotation of rigid elliptical cylinders in viscous simple shear flow: analogue experiments: *Journal of Structural Geology*, **23**, 609-617.
- Marshak, S. & Flöttman, T., 1996. Structure and origin of the Fleurieu and Nackara Arcs in the Adelaide fold-thrust belt, South Australia: salient and recess development in the Delamerian Orogen. *Journal of structural geology*, **18**, 891-908.
- Masuda, T., Michibayashi, K., and Ohta, H., 1995. Shape preferred orientation of rigid particles in a viscous matrix: re-evaluation to determine kinematic parameters of ductile deformation: *Journal of Structural Geology*, **17**, 115-129.
- Offler, R., Fleming, P.D., 1968. A synthesis of folding and metamorphism in the Mt. Lofty Ranges, South Australia. *J.Geol. Soc. Aust.*, **15**, 245–266.

-
- Pennacchioni, G., Fasolo, L., Cecchi, M.M., and Salasnich, L., 2000. Finite element modelling of simple shear flow in Newtonian and non-Newtonian fluids around a circular rigid particle. *Journal of Structural Geology*, **22**, 683-692.
- Shah, S. Z., Sayab, M., Aerden, D., & Khan, M. A. (2011). Foliation intersection axes preserved in garnet porphyroblasts from the Swat area, NW Himalaya: A record of successive crustal shortening directions between the Indian plate and Kohistan–Ladakh Island Arc. *Tectonophysics*, **509(1)**, 14-32.
- Steinhardt, C., 1989. Lack of porphyroblast rotation in non-coaxially deformed schist from Petrel Cove, South Australia, and its implication. *Tectonophysics*, **158**, 127-140.
- ten Grotenhuis, S.M., Passchier, C.W., and Bons, P.D., 2002. The influence of strain localisation on the rotation behaviour of rigid objects in experimental shear zones. *Journal of Structural Geology*, **24**, 485-499.
- Von der Borch, C. C., 1980. Evolution of the late Proterozoic Adelaide Fold Belt, Australia: comparisons with post-Permian rifts and passive margins. *Tectonophysics*, **70**, 115-134.

- CHAPTER I -

PORPHYROBLAST ROTATION VERSUS NON-ROTATION:

CONFLICT RESOLUTION!

- CHAPTER I -

PORPHYROBLAST ROTATION VERSUS NON-ROTATION: CONFLICT RESOLUTION!

ABSTRACT..... 11

I - INTRODUCTION..... 12

II – APPROACH AND RESULTS 14

III - INTERPRETATION 15

IV - DISCUSSION 16

 IV – 1 .The original geometric model..... 16

 IV – 2 .Gyrostasis 17

V - SIGNIFICANCE 18

VI – REPLY TO BONS ET AL. (2008) COMMENT 19

ACKNOWLEDGEMENT 20

ANNEX 20

REFERENCES 21

ABSTRACT

Data on foliation intersection/inflection axes preserved in porphyroblasts (FIAs) show that no porphyroblast rotation occurs during ductile deformation relative to spatial coordinates. This contrasts with 99% of investigations of “rigid” objects in non-coaxially deforming media where the objects rotate. When anastomosing shear zone formation around relatively strong objects in a weaker matrix is modelled, no “porphyroblast” rotation occurs. Formation of these anastomosing zones controls the development of this phenomenon, labelled “gyrostatics”. If such zones are absent, porphyroblasts rotate. In weak materials the gyrostatic situation arises because the superposition of simple shearing deformation normal to initial coaxial shortening results in only small rotations of principal axes of stress. Since shear zones are controlled by the orientations of principal axes of stress, initial anastomosing zones retain their orientations and positions during subsequent non-coaxial deformation. The porphyroblast is isolated from the embedding non-coaxially deforming material and material close to the porphyroblast continues to deform coaxially; no local rotation occurs. This has major significance since porphyroblasts can be routinely used to access lengthy tectonic histories destroyed in the matrix by reactivation. In particular, changes in relative directions of bulk shortening, associated with orogenesis, can now be determined within ancient orogens.

Keywords: Shear sense, porphyroblast continuum modeling, millipede microstructures, FIAs.

I - INTRODUCTION

Numerous theoretical, analogue and numerical investigations of the kinematics of rigid objects embedded in deforming rocks have been conducted (e.g., Jeffery, 1922; Ghosh and Ramberg, 1976; Ferguson, 1979; Ildefonse et al., 1992; Jezek, 1994; Masuda et al., 1995; Pennacchioni et al., 2000; Marques and Coelho, 2001; ten Grotenhuis et al., 2002; Ghosh et al., 2003; Jiang and Williams, 2004; Griera et al. 2013). They concluded that large rigid objects rotate in a non-coaxially deforming medium although recognizing certain factors (e.g. incoherent matrix inclusion interfaces (Ceriani et al., 2003; Ildefonse et al. 1992), confined shear flow (Marques and Coelho, 2001; Marques et al., 2005a, 2005b), mechanical interaction between inclusions (Ildefonse et al., 1992; Jessel et al., 2002) and stain localization (ten Grotenhuis et al., 2002; Griera et al. 2011)), can reduce, prevent or even invert rotation. These results conflict with one strain field model (Bell, 1985), partially with one experimental model (Stewart, 1996, 1997), and with a large amount of data on the orientation of foliations and foliation intersection/inflection axes preserved within porphyroblasts (FIAs) that has been published since about 1995 (Bell and Hickey, 1997; Bell and Mares, 1999; Bell and Chen, 2002; Aerden, 2004; Bell et al. 2004, 2005; Ham and Bell, 2004; Yeh and Bell, 2004; Cihan and Parsons, 2005; Sayab, 2005, 2006; Bell and Newman, 2006; Yeh, 2007; Aerden et al., 2010). Yet some authors have inferred (Jiang and Williams, 2004) that non-rotation of porphyroblasts during non-coaxial deformation is mechanically impossible in a continuum. Clearly, reconciling the bulk of the theoretical, analogue and numerical investigations with the FIA data measured in rocks needs resolution.

One characteristic of deformed rock that has not been modelled in analogue and numerical investigations and most theoretical studies with regards to porphyroblast rotation is the role of anastomosing zones of progressive shearing and shortening. This

geometry was originally generated graphically based on inclusion trail geometries preserved in and around porphyroblasts called millipede structures (Bell, 1981). It provided a solution for how a general strain could develop heterogeneously in rocks. Most significantly, it was this geometry that suggested that porphyroblasts would not rotate in a non-coaxially straining environment involving a component of bulk shortening if the porphyroblasts did not deform internally. This observation led to the recognition that spiral inclusion trail geometries could form from overprinting crenulations rather than by rotation thus producing the subsequent debate (Bell, 1985; Bell and Johnson, 1989; Passchier et al., 1992).

The results presented herein show that it is possible, within a continuum, to model non-rotation of porphyroblasts in a non-coaxial deformation environment involving synchronously developed bulk shortening and shearing. In hindsight, the deformation environment produced below, where porphyroblasts do not rotate, corresponds exactly to that which characterises all regionally metamorphosed rocks. That is, deformation environments in which a component of bulk shortening develops an anastomosing shear zone geometry around the porphyroblasts as the porphyroblasts nucleate, grow or regrow (e.g., Bell et al., 2004, Bell and Bruce, 2007). This phenomenon, called *gyrostatics*, is defined as a general non-coaxial deformation in which there is no rigid object rotation due to opposing processes (e.g. opposing shear sense on conjugate high strain zone forming around any porphyroblast) balancing each other within anastomosing zones of high strain. This result has major significance for structural geologists, metamorphic petrologists and tectonocists. Porphyroblasts can be used with confidence to access information in ductilely deformed rocks that has been obliterated in the matrix concerning directions of motion, shear senses, patterns of deformation partitioning and their changes with time, detailed PT paths linked directly

to the deformation path, and the direction of relative plate motion that caused orogenesis (e.g., Bell et al., 2004; Sayab, 2005; Bell and Newman, 2006).

II – APPROACH AND RESULTS

The modelling involves representing the porphyroblasts and matrix as Mohr Coulomb materials (*see* Annex). An anastomosing geometry of shear zones is developed by coaxially shortening the material with one or more “porphyroblasts” present. This is achieved by placing one or more square portion(s) of relatively strong material in the finite element mesh and then shortening it coaxially. 35% shortening produces the minimum anastomosing geometry (Fig. 1a,b) so that no rotation occurs during subsequent shearing plus shortening experiments where the porphyroblast lay near the centre of the model. Further shortening plus shearing produces the same anastomosing millipede geometries around porphyroblasts (Fig. 1c, d) that were generated by Bell (1981). Millipedes also develop locally out in the matrix. Shear zones, as reflected by the mesh, form because of the stress concentrations generated by the porphyroblast(s) during the initial shortening phase. These shear zones remain where they formed during subsequent shearing because of the same stress concentrations around the porphyroblasts plus the mesh sensitivity of deformation arising from this form of the constitutive model (Vermeer and deBorst, 1984). Thus, irregularities reflected by the mesh concentrate future localisation. Significantly, this behaviour simulates anastomosing foliations around porphyroblasts in nature.

Synchronous shearing and bulk shortening were applied to examples of millipede geometries produced in this way. A result is shown in Fig. 1c,d. The “porphyroblast” cores take up very little of the bulk strain and no porphyroblast rotation occurs in spite of a significant bulk non-coaxial component of deformation. When the bulk-shortening component is reduced to zero the porphyroblasts still do not rotate

provided they do not undergo internal shear strain. That is, they do not rotate during deformation involving only progressive shearing (Fig. 1e,f). Figures 1e,f and 2a to 2f show that where a porphyroblast lies close to the model boundary, a more developed millipede geometry (Fig. 2g,h) is required to prevent rotation during subsequent progressive shearing with no bulk shortening component.

Competency differences of approximately one order of magnitude (e.g., cohesion values of 10^6 Pa in the matrix and 3×10^7 Pa for the porphyroblasts) and higher produced no rotation and the porphyroblasts did not strain significantly internally. At lower competencies the porphyroblasts always internally strained and rotated. With no competency difference the porphyroblasts internally deformed and the millipedes were progressively flattened. Some deformed non-coaxially although others further developed a millipede shape.

III - INTERPRETATION

In the initial stages of modelling, the creation of an anastomosing millipede geometry in the experimental strain field was attempted by combining bulk shortening and shearing; the porphyroblasts always rotated (Fig. 3a,b). Attempts to create this geometry before starting the experiment by varying the competency in the surrounding matrix also resulted in porphyroblast rotation (Fig. 3c,d). An anastomosing geometry in the mesh was finally constructed by initially coaxially shortening the model with porphyroblasts present. This approach enabled millipede geometries to be successfully reproduced at any degree of development from weak (Fig. 1a,b), to strong (Fig. 2g,h).

With a sufficiently developed anastomosing geometry the porphyroblasts never rotate during combined shearing and shortening or during shearing alone; hence the name gyrostasis for this phenomenon (Figs. 1 and 2e,f). If an anastomosing strain field is not present, the porphyroblasts rotate (Fig. 3a to d). Gyrostasis arises because the

superposition of a simple shearing deformation normal to an initial coaxial shortening does not rotate the initial principal axes of stress appreciably if the matrix material is weak as shown in Fig. 4. This follows since the angle, Θ , between the principal axis of compression, σ_1 , and the vertical y-axis in the figures is given by $\tan 2\Theta = \tau_{xy}/(\sigma_x - \sigma_y)$ where τ_{xy} is the shear stress parallel to the x-axis and σ_x , σ_y are the normal stresses in the x and y directions (Jaeger, 1969); here the x-axis is parallel to the shearing direction and the y-axis is vertical in the figures and parallel to the initial axis of shortening. Hence if we start with a coaxial shortening with $\sigma_y = \sigma_1$ and add a shear stress, τ_{xy} , parallel to the x-axis then if the material is weak so that τ_{xy} is small, then Θ is small.

Shear zones are controlled by the orientations of the principal axes of stress and in Mohr Coulomb materials form in orientations with normals at $(\pi/4 - (\varphi + \psi)/4)$ to σ_1 where φ and ψ are the friction and dilation angles respectively (Vermeer and de Borst, 1984); for the material properties used here, the normal to the shear zones is inclined at approximately 37° to σ_1 . The initial shear zones comprising the anastomosing zones retain their orientations and positions during subsequent deformation. This isolates the porphyroblast from the embedding non-coaxially deforming material so that the material close to the porphyroblast continues to deform coaxially and no local rotation occurs.

IV - DISCUSSION

IV – 1 .The original geometric model

The construction of a strain field at constant area to mimic natural millipedes (Bell, 1981) suggested that no lines defining a 2-D mesh of squares can rotate if there is no internal strain of the square, provided the mesh is kept continuous. In constructing these models, no gapping was allowed between the squares of the initial mesh and the area of each square remained the same after distortion. With this model Bell (1985; fig. 1)

found it impossible to rotate any lines within the strain field unless there was internal distortion of the squares they bounded. This led directly to the concept that porphyroblasts do not rotate during non-coaxial ductile deformation if they do not internally deform. In the models produced where a millipede was not formed initially, rotation of porphyroblasts was accommodated by a significant area increase in the shear zones that cut obliquely across the strain field as shown in Fig. 3b,d. Such a volume increase in rocks is commonly the end product of brittle deformation and the area increase in these oblique shear zones generally leads to brittle deformation in nature and thus the rotation of any rigid objects present. Foliation development in nature is mainly accompanied by a volume decrease with dissolution and removal of non platy or non fibrous minerals and concentration of the remaining platy or fibrous grains into cleavage seams (Spiess & Bell, 1996). The only volume increase in rocks around porphyroblasts that may occur during deformation is when some of the material dissolved from developing cleavage seams is locally precipitated as “pressure fringes” in porphyroblast strain shadows.

IV – 2 .Gyrostasis

Prior to achieving an anastomosing geometry in the experiments reported here, many experiments were performed where in every case the porphyroblasts rotated (e.g., Fig. 3a,b,c,d). With the creation of sufficiently anastomosing shear zones in the mesh none of the porphyroblasts rotated. The anastomosing geometry causes the matrix to deform more pervasively around the porphyroblasts. In nature, porphyroblasts nucleate at the start of deformation when the overall strain is more or less coaxial (Bell et al., 2004, Bell and Bruce, 2007). As a result millipede geometries are relatively commonly observed in one orientation when several vertical thin sections are cut around the compass. They have been found within and on the margins of porphyroblasts of most

compositions including albite (Bell and Bruce, 2007), garnet (Spiess and Bell, 1996), staurolite, andalusite and cordierite (Bell, unpublished data). Consequently, coaxial bulk shortening and the development of a weakly anastomosing strain field prior to porphyroblast growth is the normal path for porphyroblast growth. The models presented herein, where gyrostasis occurs, directly reproduce this general phenomenon observed in rocks. Bulk scale tectonic deformations in the earth's crust comprise either horizontal shortening (due to colliding plates) or vertical shortening (due to gravitational collapse or horizontal extension). Consequently, foliations tend to form vertically or horizontally in the earth's crust and be rotated to other orientations by reactivation of compositional layering or the overprinting effects of younger deformations (e.g., Bell and Newman, 2006). These experiments show that the superposition of simple shearing deformation normal to a coaxial shortening deformation does not rotate the initial principal axes of stress appreciably in a weak material as shown in Fig. 4.

V - SIGNIFICANCE

The phenomenon of gyrostasis, revealed by continuum modelling of lack of rotation of porphyroblasts during ductile deformation, resolves the long-lived conflict between experimental, theoretical and analogue modelling and data from natural rocks on FIAs. Very lengthy tectonic histories revealed by successions of FIAs in porphyroblastic rocks can now be used to separate many periods of growth of the same porphyroblastic phase and access directions of movement, shear senses and changes in the distribution of deformation partitioning with time in the orientations in which they developed relative to the surrounding rock mass (e.g., Bell et al., 2004; Bell & Newman, 2006). Extended PT paths that are directly linked to the structural path and changes in direction

of relative plate motion with time can be determined and dated allowing this history to be integrated with large-scale plate motions (Bell and Newman, 2006).

VI – REPLY TO BONS ET AL. (2008) COMMENT

Bons et al. (2008), discussed the above subsequent to its publication. They missed the fundamental point illustrated above and further in Fig. 5 that porphyroblasts do not rotate because the strain and strain-rate is partitioned into domains in the materials (Mohr-Coulomb (Fig. 5A-F) and strain-rate softening viscous materials (Fig. 5G; annex)); they occupy regions of low strain-rate. Figure 5A-F contains variously shaped “porphyroblasts” deformed at high strains under conditions most likely to cause rotation. Their lack of rotation is independent of shape and orientation. Figure 5G emphasises that boundary conditions play little role in controlling the kinematics of the porphyroblasts and, whether localisation occurs or not, is the key! The porphyroblasts sit in regions where the strain-rate is around 10^{-12} s^{-1} whereas the bulk of the deformation is taken up in surrounding shear zones where the strain-rate reaches 10^{-9} s^{-1} . This behaviour cannot occur in the models presented by Bons et al. (2008) or most other authors in the past. It is fundamental to controlling porphyroblast kinematics.

Only *interpretations* of the origin of variably oriented and spiral-shaped inclusion trails have been used to suggest porphyroblasts rotate significantly during ductile deformation of rocks. *Data* that is independent of the *interpretation of the origin of such microstructures*, such as foliation intersection/inflection axes preserved in porphyroblasts (FIAs; e.g., Bell & Mares, 1999; Cihan and Parsons, 2004; Sayab, 2005; Rich, 2006; Yeh, 2007), indicates that they do not. None of these FIA successions, matched by progressively younger ages when dated using monazite (Bell & Welch, 2002; Sanislav & Shah, 2010), can be explained if porphyroblasts rotate during ductile deformation!

ACKNOWLEDGEMENT

I acknowledge John McLellan, Cameron Huddleston-Holmes and the ARC.

ANNEX

One could question the use of Mohr-Coulomb rheology rather than viscous to model ductile deformation. The first part of the study (Fay et al., 2008) uses Mohr-Coulomb (Vermeer and de Borst, 1984) elastic-plastic models because such rheology allows strain localization into shear bands. To produce similar localization in viscous (“Newtonian” as well as “power law”) rheology (Fay et al., 2009) there was a need to use a material that was strain rate weakening as well as strain softening (Regenauer-Lieb et al., 2009).

- The material properties used for the Mohr-Coulomb models are as follows:

	Density	Bulk modulus	Shear modulus	Cohesion	Friction angle	Dilatation angle	Tensile strength
Matrix	2500	$2.6667 \cdot 10^{10}$	$1.6 \cdot 10^{10}$	$1 \cdot 10^7$	25	5	$5 \cdot 10^6$
Porphyroblast	2500	$2.6667 \cdot 10^{10}$	$1.6 \cdot 10^{10}$	$5 \cdot 10^8$	25	5	$5 \cdot 10^6$

- The elasto-viscous material used in VI is such that the viscosity at strain-rate $\dot{\epsilon}$ is given by $\eta = \eta_0 \epsilon^p \left(\frac{\dot{\epsilon}_0}{\dot{\epsilon}} \right)^q$ where η is the current viscosity, η_0 is the viscosity at a reference strain-rate $\dot{\epsilon}_0$, and p, q are strain and strain-rate softening parameters ($p=-0.8$ and $q=2.0$; initial viscosity ratio between layers and embedding medium is 10).

REFERENCES

- Aerden, D. G. A. M., 2004. Correlating deformation in Variscan NW Iberia using porphyroblasts; implications for the Ibero-Armorican Arc. *Journal of Structural Geology*, **26**, 177-196.
- Aerden, D. G. A. M., Sayab, M., & Bouybaouene, M. L. , 2010. Conjugate-shear folding: A model for the relationships between foliations, folds and shear zones. *Journal of Structural Geology*, **32**, 1030-1045.
- Bell, T.H., 1981. Foliation development: the contribution, geometry and significance of progressive bulk inhomogeneous shortening. *Tectonophysics*, **75**, 273-296.
- Bell, T.H., 1985. Deformation partitioning and porphyroblast rotation in metamorphic rocks: A radical reinterpretation. *Journal of Metamorphic Geology*, **3**, 109-118.
- Bell, T.H. and Bruce, M.D., 2007. Progressive deformation partitioning and deformation history. Evidence from millipede structures. *Journal of Structural Geology*, **29**, 18-35.
- Bell, T.H. and Chen, A., 2002. The development of spiral-shaped inclusion trails during multiple metamorphism and folding. *Journal of Metamorphic Geology*, **20**, 397-412.
- Bell, T.H., Ham, A.P., Hayward, N., and Hickey, K.A., 2005. On the development of gneiss domes. *Australian Journal of Earth Sciences*, **52**, 183-204.
- Bell, T.H., Ham, A.P., and Kim H.S., 2004. Partitioning of deformation along an orogen and its effects on porphyroblast growth during orogenesis. *Journal of Structural Geology*, **26**, 825-845.
- Bell, T. H., and Hickey, K. A., 1997. Distribution of pre-folding linear indicators of movement direction around the Spring Hill Synform, Vermont: significance for

- mechanism of folding in this portion of the Appalachians. *Tectonophysics*, **274**, 275-294.
- Bell, T. H., and Johnson, S. E., 1989. Porphyroblast inclusion trails: the key to orogenesis. *Journal of Metamorphic Geology*, **7**, 279-310.
- Bell, T.H., and Mares, V.M., 1999. Correlating deformation and metamorphism around arcs in orogens: *American Mineralogist*, v. 84, p. 1727-1740.
- Bell, T.H., and Newman, R., 2006. Appalachian orogenesis: the role of repeated gravitational collapse: In: - Styles of continental compression, Eds R. Butler and S. Mazzoli, Special Papers of the Geological Society of America, **414**, 95-118.
- Bell, T.H., and Welch, P.W., 2002. Prolonged Acadian Orogenesis: Revelations from FIA Controlled Monazite Dating of Foliations in Porphyroblasts and Matrix. *American Journal of Science*, **302**, 549-581.
- Bons, P. D., Jessell, M. W., Griera, A., Fay, C., Bell, T. H., & Hobbs, B. E. ,2009. Porphyroblast rotation versus nonrotation: Conflict resolution! COMMENT. *Geology*, **37(2)**, e182-e188.
- Ceriani, S., Mancktelow, N. S., & Pennacchioni, G. , 2003. Analogue modelling of the influence of shape and particle/matrix interface lubrication on the rotational behaviour of rigid particles in simple shear. *Journal of Structural Geology*, **25(12)**, 2005-2021.
- Cihan, M., and Parsons, A., 2005. The use of porphyroblasts to resolve the history of macro-scale structures: an example from the Robertson River Metamorphics, North-Eastern Australia. *Journal of Structural Geology*, v. 27, p. 1027-1045.
- Fay, C., Bell, T. H., & Hobbs, B. E. 2008. Porphyroblast rotation versus nonrotation: Conflict resolution!. *Geology*, **36(4)**, 307-310.

- Fay, C., Bell, T. H., & Hobbs, B. E. 2009. Porphyroblast rotation versus nonrotation: Conflict resolution!: Reply. *Geology*, **37(2)**, e188-e188.
- Ferguson, C.C., 1979. Rotations of elongate rigid particles in slow non-Newtonian flows. *Tectonophysics*, **60**, 247-262.
- Ghosh, S.K., and Ramberg, H., 1976. Reorientation of inclusions by combination of pure shear and simple shear. *Tectonophysics*, **34**, 1-70.
- Ghosh, S.K., Sen, G., and Sengupta, S., 2003. Rotation of long tectonic clasts in transpressional shear zones: *Journal of Structural Geology*, v. 25, p. 1083-1096.
- Griera, A., Bons, P. D., Jessell, M. W., Lebensohn, R. A., Evans, L., & Gomez-Rivas, E., 2011. Strain localization and porphyroblast rotation. *Geology*, **39(3)**, 275-278.
- Griera, A., Llorens, M. G., Gomez-Rivas, E., Bons, P. D., Jessell, M. W., Evans, L. A., & Lebensohn, R., 2013. Numerical modelling of porphyroblast and porphyroblast rotation in anisotropic rocks. *Tectonophysics*, **587**, 4-29.
- Ham, A.P., and Bell, T.H., 2004. Recycling of foliations during folding. *Journal of Structural Geology*, **26**, 1989-2009.
- Ildefonse, B., Sokoutis, D., and Mancktelow, N.S., 1992. Mechanical interactions between rigid particles in a deforming ductile matrix: analog experiments in simple shear-flow. *Journal of Structural Geology*, **14**, 1253-1266.
- Jaeger, J.C., 1969. Elasticity, fracture and flow. London, Methuen & Co. Ltd., 268 p.
- Jeffery, G.B., 1922. The motion of ellipsoidal particles immersed in a viscous fluid. *Proceedings of the Royal Society of London*, **A102**, 161-179.
- Jessell, M. W., & Bons, P. D., 2002. The numerical simulation of microstructure. *Geological Society, London, Special Publications*, **200(1)**, 137-147.

- Jezek, J., 1994. Software for modelling the motion of rigid triaxial ellipsoidal particles in viscous flow. *Computers and Geosciences*, **20**, 409-424.
- Jiang, D., and Williams, P. F., 2004. Reference frame, angular momentum, and porphyroblast: *Journal of Structural Geology*, **26**, 2211-2224.
- Marques, F.O., and Coelho, S., 2001. Rotation of rigid elliptical cylinders in viscous simple shear flow: analogue experiments: *Journal of Structural Geology*, **23**, 609-617.
- Marques, F. O., Taborda, R. M., & Antunes, J. V., 2005. 2D rotation of rigid inclusions in confined bulk simple shear flow: a numerical study. *Journal of Structural Geology*, **27(12)**, 2171-2180.
- Marques, F. O., Taborda, R., & Antunes, J.V, 2005. Influence of a low-viscosity layer between rigid inclusion and viscous matrix on inclusion rotation and matrix flow: a numerical study. *Tectonophysics*, **407(1)**, 101-115.
- Masuda, T., Michibayashi, K., and Ohta, H., 1995. Shape preferred orientation of rigid particles in a viscous matrix: re-evaluation to determine kinematic parameters of ductile deformation: *Journal of Structural Geology*, **17**, 115-129.
- Passchier, C.W., Trouw, R.A.J., Zwart, H.J., and Vissers, R.L.M., 1992. Porphyroblast rotation: eppur si muove? *Journal of Metamorphic Geology*, **10**, 283-294.
- Pennacchioni, G., Fasolo, L., Cecchi, M.M., and Salasnich, L., 2000. Finite element modelling of simple shear flow in Newtonian and non-Newtonian fluids around a circular rigid particle. *Journal of Structural Geology*, **22**, 683-692.
- Regenauer-Lieb, K., Hobbs, B., Ord, A., Gaede, O., & Vernon, R. (2009). Deformation with coupled chemical diffusion. *Physics of the Earth and Planetary Interiors*, **172**, 43-54.

-
- Rich, B.H., 2006. Permian shortening in the Narragansett Basin of southeastern New England, USA. *Journal of Structural Geology*, **28**, 682-694.
- Sanislav, I.V. & Shah, A.A., 2010. The problem, significance and implications for metamorphism of 60 million years of multiple phases of staurolite growth. *Journal of the Geological Society of India*, **76**, 384-398.
- Sayab, M., 2005. N-S shortening during orogenesis within the Mt Isa Inlier (NW Queensland, Australia): the preservation of early W-E trending foliations in porphyroblasts revealed by independent 3D measurement techniques. *Journal of Structural Geology*, **27**, 1445-1468.
- Sayab, M., 2006, Decompression through clockwise P-T path: implications for an early N-S shortening orogenesis in the Mesoproterozoic Mt Isa Inlier (NE Australia). *Journal of Metamorphic Geology*, **24**, 89-105.
- Spiess, R., and Bell, T.H., 1996, Microstructural controls on sites of metamorphic reaction: a case study of the inter-relationship between deformation and metamorphism. *European Journal of Mineralogy*, **8**, 165-186.
- Stewart, L.K., 1996, Behaviour of spherical rigid objects and passive markers during bulk inhomogeneous shortening of a fluid. *Journal of Structural Geology*, **18**, 121-130.
- Stewart, L.K., 1997, Experimental investigation of the effects of a fluid heterogeneity upon the motion of a rigid porphyroblast analog during bulk inhomogeneous shortening of a fluid. *Journal of Structural Geology*, **19**, 1231-1243.
- ten Grotenhuis, S.M., Passchier, C.W., and Bons, P.D., 2002, The influence of strain localisation on the rotation behaviour of rigid objects in experimental shear zones. *Journal of Structural Geology*, **24**, 485-499.

-
- Vermeer, P.A., and de Borst, R., 1984, Non-associated plasticity for soils, concrete and rocks. *Heron*, **29**, 1-64.
- Yeh, M.-W., 2007, Deformation sequence of Baltimore gneiss domes, USA, assessed from porphyroblast foliation intersection axes. *Journal of Structural Geology*, **29**, 881-897.
- Yeh, M.-W., and Bell, T.H., 2004, Significance of dextral reactivation of an E-W transfer fault in the formation of the Pennsylvania orocline, central Appalachians. *Tectonics*, **23**, TC5009, 17p.1.

- CHAPTER II -

POLYPHASE TECTONISM AND OROCLINE DEVELOPMENT

REVEALED BY SPATIAL SHIFTS IN DEFORMATION

PARTITIONING

- CHAPTER II -

**POLYPHASE TECTONISM AND OROCLINE DEVELOPMENT REVEALED BY SPATIAL
SHIFTS IN DEFORMATION PARTITIONING**

ABSTRACT.....	30
I - INTRODUCTION.....	31
II – GEOLOGICAL BACKGROUND.....	32
III – DATA FROM PORPHYROBLASTs	33
III – 1.FIA Orientation Data	34
III – 2.FIA core rim timing	35
IV –DATA FROM FOLD AXIAL PLANE TRENDS	36
Approach Used	36
V – OBSERVATION FROM AEROMAGNETIC MAP	36
VI – IGNEOUS METAMORPHIC AND DEFORMATION AGES.....	37
VI – 2.W-E trending portions of the arc	37
VI - 2.1 Kangaroo Island	37
a) Pluton ages.....	37
b) Dyke age	37
c) Deformation/metamorphic ages.....	37
VI - 2.2 Curnamona craton	37
Shear zones	37
VI – 3.N-S trending portions of the arc	38
VI - 3.1 Pluton ages	38
VI - 3.2 Dyke ages	38
VI - 3.3 Deformation/metamorphic ages	39

VII - INTERPRETATION.....	39
VII – 1.Pre-amble	39
VII – 2.FIA succession	39
VII – 3.Igneous Ages versus Orocline trends	40
VII – 4.Relationship between Fold axial planes and FIA succession.....	40
VII – 5.Aeromagnetic trends	41
VII – 6.Timing of development of the N-S versus the W-E trending trending portion of the orogen	41
VII – 7.Model for Orocline development	42
VIII - DISCUSSION.....	43
VIII – 1.Nature of the contact between the Proterozoic and Cambrian sequence	43
VIII - 2.Significance of peaks in the distribution of fold axial plane trends	44
VIII – 3.Updated model of Orocline development	45
VIII – 4 .Implications for Australian early Paleozoic tectonic history	46
ACKNOWLEDGMENT	46
REFERENCES	47

ABSTRACT

Porphyroblast microstructures in rocks from a narrow portion of the sigmoidal-shaped Adelaide geosyncline indicate that the Delamerian Orogeny was a product of five changes in the direction of bulk shortening. The progression from NNW-SSE to WSW-ENE to SSW-NNE to WNW-ESE to NNE-SSW directed bulk shortening, resulted from shifts in the direction of relative plate motion as orogenesis progressed between 522 and 478 Ma. These directions were determined from a succession of 5 FIAs (Foliation Intersection/Inflection Axes preserved within porphyroblasts). The overprinting relationships between the multiple generations of regional folds that developed were resolved using the timing criteria provided by this FIA succession. The S-shape of the orocline has been interpreted as a fold and thrust belt product of either oblique convergence or the development of asymmetric syntaxis zones but this is not the case. Rather the orocline resulted the overprinting of a succession of near orthogonal plan view changes in the direction of convergence. This reflects much of the geodynamic evolution of the Eastern Australian portion of the Gondwana margin during its early Paleozoic history.

Keywords: Kanmantoo group, Adelaide geo-syncline, Gondwana, porphyroblast, interpreting combined geophysical and geological maps, S-shape Orocline, FIAs

I - INTRODUCTION

Resolving how oroclinal folds develop and their timing has been a problem in tectonics ever since such structures have been recognized. As a result, different scenarios are commonly proposed for the development of any orocline that has been studied by several different groups. This is typified by the various models proposed for the orocline in the Adelaide geosyncline from Coward (1976), Clark & Powell (1989) and Marshak & Flöttman (1996) shown in Fig. 1 summarized from Figs 2, 10 & 12 in the latter paper. Such approaches highlight the classic structural geology problem of many solutions possible for the development of any complex structural geometry if the stages in its history of development cannot be determined. That is, most finite deformation structures can be the product of many different deformation paths.

Data on many stages in the history of development of structures can be obtained from recently developed techniques for quantitatively analyzing foliations preserved in porphyroblasts. This provides a new approach for analyzing the development of oroclinal folds because both numerical models (Fay et al., 2008, 2009; Sanislav, 2010) and quantitative data on such foliations suggests that they are not rotated by subsequent ductile deformation events (e.g., Bell & Mares, 1999; Yeh & Bell, 2004). This should include any orogens where extensive ductile shearing (Jung et al., 1999, Bell & Kim, 2004; Fay et al., 2009) was involved in orocline development. If such a phenomenon proves to apply in most orogens, and much recent data suggests that is the case (e.g., Shah et al., 2011; Bell & Sapkota, 2012; Aerden et al., 2013), it could prove to be very useful generally in resolving problems with orocline development.

Recently, it has become apparent that a succession of Foliation Intersection/Inflection Axes preserved in porphyroblasts (FIAs) can be directly linked to peaks in statistical distributions of fold axial plane trends (Abu Sharib & Bell, 2011;

Bell & Sanislav, 2011; Aerden et al., 2013). If this linkage occurs in orogens elsewhere, it will provide an approach to fold analysis that short circuits the problem of correlating foliations from outcrop to outcrop across a region. The possibility of correlation problems resulting from several foliations forming in sub-vertical and sub-horizontal orientations and intersecting in a common axis is significantly diminished. These axes, called FIAs when measured in porphyroblasts, can be readily measured. Such quantitative work in many orogens around the world has revealed that each FIA is just one in a succession of several that can be readily defined (e.g., Aerden, 2004; Cihan & Parsons, 2005; Rich, 2006; Ali, 2009; Bell & Sapkota, 2012; Cao & Fletcher, 2012; Quentin de Gromard, 2013). Most significantly, FIAs allow one to take into account the effects of differential partitioning of the deformation across an outcrop (Sanislav & Bell, 2011) or a region (e.g., Bell et al., 2013).

The research described herein uses data obtainable from any geologic/geophysical map of a terrane containing rocks locally affected by regional metamorphism to garnet or higher grades. In combination with the succession of FIAs obtained from the latter portion this has enabled resolution of the history of development of the large-scale S-shaped orocline defined by the Adelaide Geosyncline and should work for any orocline locally containing porphyroblastic rocks.

II – GEOLOGICAL BACKGROUND

The Adelaide geosyncline contains an older sequence of late Proterozoic (800-600 Ma) rocks (the Adelaidean Formation, Fig. 2) deposited in shallow water in an intracratonic rift setting provided by metamorphic basement complexes of the Gawler craton (Preiss 1987). It also contains a thick younger early-Cambrian flysch-like sequence (Daily & Milnes, 1973; Von der Borch, 1980) called the Kanmantoo Group. The boundary

between these units locally contains a tuffaceous layer dated at 526 ± 4 Ma (Cooper et al., 1992).

The effects of deformation appear to have resulted from the Delamerian Orogeny with a synorogenic I-S type granite dated at 516 Ma and undeformed A-type granite and gabbros dated around 486 Ma (Foden et al., 1990; Sandiford et al., 1992). In Fig. 2 the Adelaide geosyncline appears relatively simple with open gently doubly plunging folds rotating from N-S trends in the centre to W-E trends to the N around the Nackara Arc and to the S around the Fleurieu Arc (Fig. 2). A slaty cleavage increases in intensity of development from W to E across the Nackara Arc (Bell, 1978) and is commonly preserved in rocks along the N-S trending central portion. Later generations of locally well-developed crenulation cleavage are commonly developed within higher grade metamorphic rocks, especially in the Kanmantoo region to the east of Adelaide and also on the W-E trending portion of the Fleurieu Arc (Fig. 2; Mills, 1964; Offler, 1966; Offler and Fleming, 1968; Fleming, 1971; Steinhardt, 1989; Adshead-Bell & Bell, 1999). In Buchan low-grade metamorphic terranes within in the Adelaidean, the deformation remains simple at both macroscopic, mesoscopic and microscopic scales. The higher metamorphic grade (amphibolite facies with kyanite-sillimanite bearing metapelites) Kanmantoo Group displays a macroscopic deformation pattern that is concordant with the general N-S trend of the orogen (Fig. 3). However, mesoscopic investigations reveal a more complex deformation history with evidence for three or four foliations (S_1 , S_2 , S_3 , S_4) visible in the outcrop (e.g., Mills, 1964; Offler, 1966; Offler and Fleming, 1968; Fleming, 1971).

III – DATA FROM PORPHYROBLASTS

59 samples were collected within the Kanmantoo formation about 50 km East of Adelaide (Fig. 3). The regional foliation trends N-S and dips steeply towards the east.

Of these 59 samples, 40 contain porphyroblasts. Six vertical thin sections 30° apart were cut from each of these. These metapelitic samples most commonly contain staurolite (Fig. 4a, b), andalusite (Fig. 4b) and garnet (Fig. 4a) porphyroblasts plus rare coarse muscovite pseudomorphs after cordierite. In thin section the foliation, which is mainly defined by aligned biotite and muscovite grains (locally associated with chlorite or sillimanite) forms anastomosing arrays that partition the matrix into domains of high strain and low strain (Fig. 4b).

Andalusite occurs as large poikilitic and anhedral porphyroblasts. Staurolite is present as poikilitic and anhedral to euhedral porphyroblasts (commonly twinned). Their size varies from one millimeter to one centimeter. Staurolite porphyroblasts occur as large crystals and locally as inclusions within andalusite porphyroblasts. Garnet porphyroblasts are rounded to euhedral occurring both in the matrix and as inclusions within staurolite and andalusite porphyroblasts. The inclusion trails are defined by the alignment of elongate shaped quartz and ilmenite grains. Although in some section orientations, inclusion trails may appear continuous with the matrix foliation in porphyroblast strain shadows, when examined in 3-D using all 6 thin sections most are actually truncated (Fig. 4). Based on core to rim and porphyroblast-matrix relationships, at least 4 generations of staurolite, 4 of andalusite, and 4 of garnet can be inferred (see below).

III – 1.FIA Orientation Data

The axis of curvature of a foliation defined by inclusion trails that curve sigmoidally or which run straight across a porphyroblast core and curve only within its the rim, or the intersection of 2 foliations, defines a FIA. The dominance of sub-vertical and sub-horizontal inclusion trails in vertical rose diagrams, wherever quantitative data is obtained (Hayward, 1992; Aerden, 2004; Bell & Sapkota, 2012), suggests that this axis

is the product of successive sub-vertical and sub-horizontal bulk shortening (e.g., Bell & Johnson, 1989). Each FIA trend is governed by the strike of any vertical foliations preserved as inclusions within a porphyroblast (Bell & Sanislav, 2011). The FIA is located between the two thin sections where the curvature of the inclusion trails switches asymmetry (e.g., clockwise to anticlockwise as shown in Hayward, 1990; Bell et al., 1995; 1998). Measurement of the FIAs was attempted using the 6 thin-sections cut from each of the 40 samples mentioned. Of the initial 240 thin sections prepared only those from 24 of the 40 contained sufficiently well-defined inclusion trails to measure FIAs. However, 49 FIAs were measured within 10° from these 24 samples by cutting between 2 and 10 extra thin sections per sample. These FIAs cluster into a well-defined distribution of trends (Fig. 5). The total FIAs measured (Fig. 5a) from staurolite (20 Fig. 5b), andalusite (22 Fig. 5c) and garnet (7; Fig. 5d) define 5 peaks trending WNW-ESE, NNW-SSE, SSW-NNE, SW-NE and WSW-ENE.

III – 2.FIA core rim timing

A porphyroblast core forms before its rim. Consequently, changes in FIA trend from the core to the rim reveal the relative timing of different FIA trends in that sample. Such changes in FIA trend are documented in Fig. 6a. A comparison of Fig. 6b with Fig. 6a suggests a consistent succession of FIA trends is present (see below). Figure 6c is a table showing all FIAs measured, their host phase, FIA set in the succession from Fig. 6b and location relative to core, median or rim trails. Only nine out forty nine (~18%) samples bear more than a singular FIA. However it is routinely noted that timing criteria for FIAs are always limited (Bell et al., 1998) the maximum being 30% of samples containing multiple FIAs.

IV – DATA FROM FOLD AXIAL PLANE TRENDS

Approach Used

1. Refolded and overprinted folds are readily observed on regional geological maps and in many cases also on aeromagnetic and radiometric maps when studied in detail. Figures 7 and 8 show geological (a), aeromagnetic (b) and radiometric (c) maps of the Nackara and Fleurieu arc regions respectively. On overlays of each map, the geological or geophysical boundaries defining folds were drawn and combined in Figs 7d & 8d on which the various geological and geophysical boundaries are marked with different colors. The axial planes of these folds were then marked on each of these overlays and are highlighted on the larger maps shown in Figs 9 & 10. The trends of every axial plane were measured using IMAGE J software.

2. Folds that overprint others provide timing criteria. Refolds combined with wrong sense asymmetry folds on one of the earlier formed fold limbs provide timing criteria between any 2 generations of folds (Fig. 11a, b). These were distinguished for examples of re-fold structures visible in detail on the maps (e.g., Figs 9 & 10).

3. The axial plane data are plotted on the rose diagram in Fig. 12.

4. This can then be compared with the distribution of FIAs (Fig. 6a).

V – OBSERVATION FROM AEROMAGNETIC MAP

The aeromagnetic map shown in Fig. 13 shows an $\sim 345^\circ$ trending portion of the fold belt that extends well to the North and South of the W-E trending portions of the Nackara and Fleurieu Arcs. This has considerable significance and is interpreted and discussed in some detail below.

VI – IGNEOUS METAMORPHIC AND DEFORMATION AGES**VI – 2.W-E trending portions of the arc***VI - 2.1 Kangaroo Island**a) Pluton ages*

The Kanmantoo group rocks on Kangaroo Island are intruding by a numerous granitoids (Fig. 14a). The ages of the emplacement of these I-S type granites range from 522 ± 5.7 Ma (Flöttman et al., 1995) to 503 ± 4 Ma (Burt & Fanning, PIRSA database). Igneous zircon ages have also been obtained comprising 511 ± 3 Ma (in a Kangaroo Island pegmatite, Drexel & Preiss, 1995), 508 ± 7 Ma and 509 ± 7 Ma (deformed granite parallel to the turbiditic bedding on Cape Willoughby; Drexel & Preiss, 1995) and Fanning (1990), respectively; and 504 ± 8 Ma (from a megacrystic granite in Vivonne Bay, Fanning, 1990). The Encounter bay granite, which outcrops on the mainland, maintains the 075° trend of those on Kangaroo Island and has been dated at 504 ± 8 Ma (Rb-Sr, Drexel & Preiss, 1995).

b) Dyke age

On Cape Gantheaume, steeply dipping composite dykes between 0.5 and 4m wide and trending around 325° contain zircons dated at 500 ± 7 Ma (Fanning, 1990).

c) Deformation/metamorphic ages

The youngest age found on Kangaroo Island consist of a two mica/apatite Rb-Sr age at 487 ± 3.5 Ma at Vivonne bay (Foden et al., 2002b) interpreted as a cooling age.

*VI - 2.2 Curnamona craton**Shear zones*

The western margin of the Curnamona craton (Fig. 2) contains W-E trending Delamerian shear zones. Monazites from within these shear zones and in the surrounding kyanite bearing schist have U-Th-Pb ages ranging from 508 ± 15 to 497 ± 22

Ma (Dutch et al. 2005). These shear zone ages appear to be consistent with those on Kangaroo Island associated with granitoid emplacement but have a large error range. Figure 14b shows a histogram of these ages. They lie predominantly between 522 and 497 Ma.

VI – 3.N-S trending portions of the arc

VI - 3.1 Pluton ages

This portion of the arc has been intruded by a variety of granitoids and bimodal dykes (Fig. 14a). The Rathjen gneiss, which contains magmatic zircons dated at 514 ± 5 Ma (Foden et al., 1999) was followed by a series of magmatic bodies that are some 20 million years younger. The Monarto granite has a monazite age at 492.8 ± 1.3 Ma (Foden et al., 2006) similar to the Palmer granite at 490 ± 4 Ma (Turner, 1996) and the Reedy Creek magmatic series at 491 ± 1 Ma (diorite) and 490 ± 2.1 Ma (granodiorite; Foden et al., 2006). The youngest granitoid ages for this portion of the arc are the Mannum granite dated by Rb-Sr at 482.3 ± 4.5 Ma (Turner & Foden, 1996) and the Kinchinna quarry pegmatite dated at 478 ± 2 Ma (Burt & Philips, 2003).

The Padthaway Ridge to the east of the Kanmantoo region, which has NNE-SSW trends contains the Marcollat Granite with a titanite age from syenite at 488.7 ± 3.7 Ma (Foden et al., 2006). To its North-East lies the Anabama granite dated at 485.7 ± 3.5 Ma (Foden et al., 2002b).

VI - 3.2 Dyke ages

The earliest dyke is a meta-dolerite dated at 510 ± 2 Ma at Tungkillo (Chen & Liu, 1996; Fig. 14a). The Reedy Creek granite is intruded by rhyolite dykes dated at 486 ± 0.5 Ma (Foden et al., 2006). An undeformed gabbro at Black Hill has an age of 487 ± 5 Ma (Milnes et al., 1977).

VI - 3.3 Deformation/metamorphic ages

A metamorphic rim on a zircon has been dated at 503 ± 7 Ma in the Rathjen Gneiss (Foden et al., 1999). A younger migmatite was dated at 480 ± 4 Ma in Reedy Creek (Turner et al., 1996). Figure 14c shows a histogram of these ages. They differ from Fig. 14a in that they contain many ages between 500 and 478 Ma. The combined distribution on a histogram of all the above ages is shown in Fig. 15.

VII - INTERPRETATION

VII – 1.Pre-amble

FIA's obtained from a limited area within the NE Appalachian orogen where porphyroblast growth dominates have been recently shown to reflect regional fold axes on a much larger scale along the orogen (Bell & Sanislav, 2011). These authors argued that porphyroblast growth becomes significant during regional metamorphism at around 520-540°C. This heat, plus the contrast in competency with the rock matrix that porphyroblasts provide, appears to result in most deformations, and the effects of metamorphism that accompanies each event, being partitioned to some degree through this location. In other words hotter regions generally show the impact of deformation associated with all regional changes in bulk shortening preserved as FIA's because strain within the less competent matrix is preferentially localized against competent porphyroblasts.

VII – 2.FIA succession

In sample 21, the WSW-ENE FIA in garnet cores predates the NNW-SSE trending garnet FIA (Fig. 6b). NNW-SSE trending FIA's lie in the cores of porphyroblasts with WNW-ESE and SSW-NNE FIA trends in their rims (Fig. 6b) and thus predate them. WNW-ESE FIA in staurolite cores predate SSW-NNE FIA in staurolite rims (Fig. 6b).

WNW-ESE and SSW-NNE FIAs lie in the cores of porphyroblasts with SW-NE rim trends. Therefore, the SW-NE FIA is the youngest.

Thus Fig. 6b reveals a consistent FIA succession from WSW-ENE, NNW-SSE, WNW-ESE, SSW-NNE to finally SW-NE.

VII – 3. Igneous Ages versus Orocline trends

W-E trending portions of the orocline are dominated by 520 to 497 Ma plutons and deformation ages (Fig. 14b). The N-S trending portion of the orocline contains 514 and 510 Ma igneous ages and one metamorphic rim age around 503 Ma, but is dominated by 492 to 480 Ma igneous and deformation ages (Fig. 14c). This suggests that it contains relics of the pre 495 Ma igneous and deformation history observed in the W-E trending portions of the Orocline but has been strongly affected by younger periods of orogenesis that generated granites and higher grade metamorphic effects from 492 to 487 Ma that did not affect at all or had little impact on the W-E trending portions.

VII – 4. Relationship between Fold axial planes and FIA succession

The comparison of Figs 6 and 12 shown in Fig. 16 indicates significant correspondence in most peaks in the distribution of fold axial plane trends with those in FIAs. This provides an approach to interpreting the timing of successive regional fold events after the manner and reasoning described in Bell & Sanislav (2011) whereby the peaks in the distribution of axial plane trends may directly reflect the FIA succession. It potentially allows one to test the validity of the FIA succession through fold overprinting criteria at smaller regional scales. At the latter scales wrong sense asymmetries and other interference criteria suggest a series of overprinting relationships. The following succession of fold generations can be observed:

1. A generation of WSW-ENE fold axial plane traces are overprinted by a generation of folds with NNW-SSE axial planes (Fig. 16b, LHS rose diagram) matches the succession of shortening directions suggested by the shift from FIA I to FIA II.
2. Folds with N-S trending axial planes refolded by folds with E-W trending axial planes (Fig. 16b, RHS rose diagram) is consistent with the shift from FIA II to FIA III.
3. Where multiple sets of overprinting folds are observed, the tectonic reconstruction is a lot more difficult. Indeed the latest fold axial plane orientation could be a product of incremental variable rotation of the fold limbs over several deformation events (Fig. 16c).

VII – 5. Aeromagnetic trends

The aeromagnetic map in Fig. 13 shows that the 345° trending portion of the Adelaide Geosyncline overprints W-E trending portions of the Fleurieu and Nackara Arcs. This suggests that the orogen trended around WSW-ENE before the 345° trending central portion was formed as shown in Fig. 17. This is strongly supported by the fact that FIA I trends at approximately $75^{\circ} \pm 15^{\circ}$ and the subsequent FIA II trends at $170^{\circ} \pm 5^{\circ}$ and so bulk shortening would have been directed initially NNW-SSE and then ~W-E.

VII – 6. Timing of development of the N-S versus the W-E trending trending portion of the orogen

The FIA succession, igneous and deformation age relationships and truncational character on the aeromagnetic map of the N-S relative to W-E trending portions of the orocline indicate that the W-E trending portion formed first between 520 and 495 Ma and was rotated after 494 Ma to more N-S trends by at least 2 periods of overall W-E bulk shortening that produced NNW-SSE and SSW-NNE trending FIAs.

VII – 7. Model for Orocline development

Figure 17a shows the orogen trending around WSW-ENE. Figure 17b shows the impact of approximately W-E bulk shortening on Fig. 17a. This rotates the orogen into a NNW-SSE orientation (as shown in Fig. 17b). This was aided by the presence of the Gawler Craton. This competent mass prevented deformation during ~W-E bulk shortening from partitioning through it and resulted it localizing to the east. The FIA succession and succession of trends allows one to suggest what caused the succession of orogen trends. The first FIAs formed in garnet porphyroblasts with a trend of $\sim 75^\circ$, indicating bulk shortening trending $\sim 165^\circ$ (Fig. 17c). This would have produced $\sim 75^\circ$ trending folds and contributed to the ~W-E trend of the initial orogen. The subsequent period of bulk shortening was directed at 75° because it formed FIAs trending at 165° in staurolite and andalusite (Fig. 17d). This could have rotated the orogen to an ~N-S trend because of partitioning of the deformation against the edge of the Gawler craton, possibly aided by the present of the Curnamona craton to the east. This period of ~W-E bulk shortening that was accompanied by staurolite and andalusite growth was the earliest period of growth of these porphyroblastic phases.

The later changes in the direction of bulk shortening associated with the development of FIAs III, IV and V had limited effects on the overall geometry of the orocline. During the N-S bulk shortening that accompanied staurolite and andalusite growth during FIA III, the presence of the competent Gawler craton to the west would have protected in its strain shadow the rocks in the N-S trending portion of the orogen. This would explain the relative paucity of large-scale folds resulting from this period of bulk shortening. During the W-E bulk shortening that accompanied staurolite and andalusite growth during FIA IV, strain would have been localized against the protruding SE corner of the rigid Gawler craton. This may explain the heterogeneity in

intensity of ~ N-S trending deformation in the N-S trending portion to the east of Kangaroo Island (Fig. 13). That and the presence of numerous plutons may explain the increased heterogeneity in this region that appears to be associated with the development of FIA V.

VIII - DISCUSSION

VIII – 1. Nature of the contact between the Proterozoic and Cambrian sequence

Lithospheric scale thrusts and folds were proposed in a model that would make the Kanmantoo an allochthonous tectono-metamorphic block accreted nappe-like onto the Adelaidean (Jenkins & Sandiford, 1992; Flöttman et al. 1994, 1997). Direen et al. (2005) used forward magnetic geophysical modeling in an attempt to validate the thrusts proposed by Flöttman et al. (1994). They found significant differences between the modeled effect and the measured anomaly as shown in Fig. 18 that strongly suggest problems with this thrust interpretation of these cross-sections. Indeed, major thrusting of the Kanmantoo to the West should produce a progressive rotation of crenulation cleavages lying axial plane to regional folds from sub-vertical at higher crustal levels to sub-horizontal towards the thrust plane. Yet Fig. 19 shows that the dips of this cleavage are predominantly close to sub-vertical around the potential thrust. It appears that thrusting as envisaged by Flöttman (1994) did not occur.

This conclusion is strongly supported by the fact that metapelite samples collected from the Precambrian and Cambrian sequences to either side of Flöttman's (1994) thrust are very similar in metamorphic grade containing similar staurolite, andalusite and sillimanite assemblages (e.g., samples 42 and 43, Fig. 3). In addition the combination of the radiometric, aeromagnetic and geological maps highlights the lack of structural hiatus between the Cambrian and Proterozoic sequences (Fig. 20). The Kanmantoo group is thus either conformable on the Adelaidean supergroup or was

tectonically superposed prior to the regional upright folding event, for which there is no evidence.

VIII - 2. Significance of peaks in the distribution of fold axial plane trends

Fold axial plane trends will vary significantly in their totality relative to FIA trends spreading widely on rose diagrams because each generation of folds will be rotated by those formed subsequently. However, Bell & Sanislav (2011) and Abu Sharib & Bell (2011) have shown that peaks in the distribution of fold axial plane trends from regional maps strongly mimic FIA trends. This correlation already noted by Aerden et al. (2004, 2013), suggests that deformation never partitions pervasively across a region and relics of portions of even the first formed generation of folds are left preserved in their original orientation across a region. Further, even if one fold is overprinted by another younger fold generation, somewhere in the redistribution of original fold axial plane trend lays the original orientation of that fold (e.g., Bell & Sanislav, 2011). This applies for every successive event. One could expect early-formed folds to soon disappear. However, first formed folds commonly form with very large wavelengths and amplitudes because the basin layering is unfolded and beds are thick (Bell et al., 2003). Furthermore, because deformation partitioning always takes place, portions of each successive deformation event are left unaffected by all subsequent events in some locations. In the case of the Adelaide geosyncline, this is most obvious in the W-E trending portion of the Fleurieu Arc where schistosity parallel to layering trends ~W-E and is overprinted by folds with axial planes trending WSW-ESE strain zones still trend at approximately 75° sub-parallel to FIA I (Fig. 21). Indeed Weinberg et al., 2013 describe several deformation events, most of which possibly formed during the development of FIA I.

VIII – 3. Updated model of Orocline development

The formation of S shaped oroclinal arcs has long been puzzling with most present day models involving oblique convergence or the development of asymmetric syntaxis zones (Coward, 1976; Clarke & Powell, 1989; Marshak & Flöttmann, 1996). The scenarios proposed to explain the Fleurieu/Nackara arc orocline involve tangential sinistral NW trending shear zone (Fig. 1a, Coward, 1976), transpression between zones of shearing on E-W-trending dextral strike-slip faults (Fig. 1b, Clarke & Powell, 1989) and W-E compression against the Gawler craton (Fig. 1c, Marshak & Flöttmann, 1996).

It has been shown herein that the shape of Adelaide Geosyncline was a product of a succession of bulk shortening events generally at successively high angles to each other around the compass except for the last FIA to form (Fig. 6a). The W-E to WSW-ENE trending folds preserved on Kangaroo Island and the Northern part of the belt were formed by a long period of ~N-S bulk shortening from 520 to around 495 Ma. The whole region then experienced ~W-E bulk shortening that formed the folds with an upright NNW-SSE orientation (Fig. 17). The three changes in subsequent bulk shortening events, which generated FIAs III, IV and V had little large scale effects on the overall shape of the orogen but formed numerous refolds with it. Large wavelength and amplitude regional folds probably formed early because prior to their development, the well developed and preserved bedding containing numerous competent horizons was relatively layer cake and flat lying to gently dipping (Biot, 1961; Bell et al., 2003). In conclusion, the major orogenic features were produced in the early stages of the Delamerian orogenic cycle.

VIII – 4 .Implications for Australian early Paleozoic tectonic history

On a bigger scale the footprint of the Delamerian Orogeny is interpreted by many as having a large geographical extent across the Australian continent. A metamorphic event at 490+8 Ma has been dated in the Georgetown Inlier (Nishiya et al., 2003). This suggests that part of the early Thompson Orogeny deformation to the East is the result of the same W-E convergence event responsible of the N-S general trend of the Adelaide geosyncline (Fergusson et al., 2007b, 2007b). Quentin De Gromard (2013) highlighted the repetitive episodic cycling of N-S bulk shortening events and W-E bulk shortening events from 470 Ma onwards in the Charters Towers province. The tectonic model proposed for the Adelaide geosyncline, supported by the FIA succession from the Kanmantoo region, is consistent with such episodic repetitions of N-S and E-W bulk shortening events having started well before that period in the late Cambrian. Thus the entire Eastern Gondwana active margin that is preserved within Australia experienced multiple successions of bulk shortening that switched from ~N-S to ~E-W during the numerous periods of deformation that accompanied orogenesis in most of the Paleozoic.

ACKNOWLEDGMENT

T.H.Bell , I.V. Sanislav, A. Ali, T. Blenkinsop , R.A. Henderson, M.J. Rubenach

REFERENCES

- Abu Sharib, A.S.A.A., Bell, T.H., 2011. Radical changes in bulk shortening directions during orogenesis: significance for progressive development of regional folds and thrusts. *PreCambrian Research*, **188**, 1-20.
- Adshead-Bell, N.S. & Bell, T.H., 1999. The progressive development of a macroscopic upright fold pair during five near orthogonal foliation production events: complex microstructures versus a simple macrostructure. *Tectonophysics*, **306**, 121-147.
- Aerden, D.G.A.M., 2004. Correlating deformation in Variscan NW Iberia using porphyroblasts; implications for the Ibero-Armorican Arc. *Journal of Structural Geology*, **26**, 177–196.
- Aerden D.G.A.M., Bell T.H., Puga E., Sayab M., Lozano J.A. & Diaz de Federico A., 2013. Multi-stage mountain building vs. relative plate motions in the Betic Cordillera deduced from integrated microstructural and petrological analysis of porphyroblast inclusion trails. *Tectonophysics*, **587**, 188-206.
- Ali, A., 2010. The tectono-metamorphic evolution of the Balcooma Metamorphic Group, northeastern Australia; a multidisciplinary approach. *Journal of Metamorphic Geology*, **28**, 397-422.
- Bell, T. H., 1978. The development of slaty cleavage across the Nackara Arc of the Adelaide Geosyncline. *Tectonophysics*, **51**, 171-201.
- Bell, T.H., Forde, A. & Wang, J., 1995. A new indicator of movement direction during orogenesis: measurement technique and application to the Alps. *Terra Nova*, **7**, 500-508.
- Bell, T. H., Hickey, K. A., & Upton, G. J. G., 1998. Distinguishing and correlating multiple phases of metamorphism across a multiply deformed region using the

- axes of spiral, staircase and sigmoidal inclusion trails in garnet. *Journal of Metamorphic Geology*, **16**(6), 767-794.
- Bell, T.H., Ham, A.P. & Hickey, K.A., 2003. Early formed regional antiforms and synforms that fold younger matrix schistosity: their effect on sites of mineral growth. *Tectonophysics*, **367**, 253-278.
- Bell, T.H., Ham, A.P., Kim H.S., 2004. Partitioning of deformation along an orogen and its effects on porphyroblast growth during orogenesis. *Journal of Structural Geology*, **26**, 825-845.
- Bell, T.H. & Hickey, K.A., 1998. Multiple deformations with successive sub-vertical and sub horizontal axial planes: their impact on geometric development and significance for mineralization and exploration in the Mount Isa region. *Economic Geology*, **93**, 1369-1389.
- Bell, T.H. & Johnson, S.E., 1989. Porphyroblast inclusion trails: the key to orogenesis. *Journal of Metamorphic Geology*, **7**, 279-310.
- Bell, T.H. & Kim, H.S., 2004. Preservation of Acadian deformation and metamorphism through intense Alleghanian shearing. *Journal of Structural Geology*, **26**, 1591-1613.
- Bell, T.H. & Mares, V.M. 1999. Correlating deformation and metamorphism around orogenic arcs. *American Mineralogist*, **84**, 1727-1740.
- Bell, T.H., Rieuwers, M.T., Cihan, M., Evans, T.P., Ham, A.P., Welch, P.W., 2013. Inter-relationships between deformation partitioning, metamorphism and tectonism. *Tectonophysics*, **587**, 119-132.
- Bell, T.H. & Sanislav, I.V., 2011. A deformation partitioning approach to resolving the sequence of fold events and the orientations in which they formed across

- multiply deformed large-scale regions. *Journal of Structural Geology*, **33**, 1206-1217.
- Bell, T.H., Sapkota, J., 2012. Episodic gravitational collapse and migration of the mountain chain during orogenic roll-on in the Himalayas. *Journal of Metamorphic Geology* **30**, 651-666.
- Burt, A. C.; Abbot, P. J.; and Fanning, C. M. 2000. Definition of Teal Flat and Marne River Volcanics and associated shear zone. *MESA J.*, **17**, 37–43.
- Burt, A. C., and Phillips, D. 2003. Ar/Ar dating of a pegmatite, Kinchina Quarry, Murray Bridge, *South Australia*. *MESA J.* , **28**, 50–52.
- Biot, M.A., 1961. Theory of folding of stratified viscoelastic media and its implications in tectonics and orogenesis. *Geol. Soc. Amer. Bull.* , **72**, 1595– 1620.
- Cao, Hui, and Fletcher, Chris (2012) Using foliation inflection/intersection axes investigates orogenesis: take Arkansas River region, USA for example. *Yanshi Xuebao* , **28** ,1937-1948.
- Chen, Y.D., Liu, S.F., 1996. Precise U-Pb zircon dating of a post-D2 meta-dolerite: constraints for rapid tectonic development of the southern Adelaide Fold Belt during the Cambrian. *Journal off the Geological Society, London*, **153**, 83-90.
- Cihan, M. & Parson, A. 2005. The use of porphyroblasts to resolve the history of macro-scale structures: an example from the Robertson River Metamorphics, North-Eastern Australia. *Journal of Structural Geology*, **27**, 1027–1045
- Clarke, G. L. & Powell, R. 1989. Basement/cover interaction in the Adelaide Foldbelt, South Australia: the development of an arcuate foldbelt. *Tectonophysics* , **158**, 209-226.

- Cooper, J.A., Jenkins, R.J.F., Compston, W. and Williams, I.S., 1992. Ion-probe zircon dating of a mid-Early Cambrian tuff in South Australia. *J. Geol. Soc. London* , **149**, 185-192.
- Coward, M. P. 1976. Large scale Palaeozoic shear zone in Australia and present extension to the Antarctic Ridge. *Nature* , **259**, 648-649.
- Direen, N.G, Brock, D. Hand, M., 2005. Geophysical testing of balanced cross-sections of fold–thrust belts with potential field data: an example from the Fleurieu Arc of the Delamerian Orogen, South Australia. *Journal of Structural Geology* , **27**, 964–984.
- Dutch, R.A., Hand, M., Clark, C. 2005. Cambrian reworking of the southern Australian Proterozoic Curnamona Province: constraints from regional shear-zone systems. *Journal of the Geological Society* , **162**, 763-775.
- Daily, B. & Milnes, A. R. 1973. Stratigraphy, structure and metamorphism of the Kanmantoo Group (Cambrian) in its type section east of Tungkillia Beach, South Australia. *Trans. R. Soc. S.Aust.* , **97**, 213-242.
- Drexel, J. F., and Preiss, W. 1995. The geology of South Australia. Vol. 2. The Phanerozoic. S. Aust. Geol. Surv. Bull. 54.
- Fanning, C. M. 1990. Single grain dating of a granite sample from Cape Willoughby, Kangaroo Island. *Prise Laboratories, Australian National University Progress Report 89-060*. S. Aust. Dept. of Mines and Energy, Open File Envelope 8828:29–32.
- Fay, C., Bell, T. H., & Hobbs, B. E. 2008. Porphyroblast rotation versus nonrotation: Conflict resolution!. *Geology*, **36(4)**, 307-310.
- Fay, C., Bell, T. H., & Hobbs, B. E. 2009. Porphyroblast rotation versus nonrotation: Conflict resolution!: Reply. *Geology*, **37(2)**, e188-e188.

- Fergusson, C.L., Henderson, R.A., Withnall, I.W., Fanning, C.M., Phillips, D., Lewthwaite, K.J., 2007a. Structural ,metamorphism and geochronological constraints on alternating compression and extension in the Early Paleozoic Gondwanan Pacific margin, northeastern Australia. *Tectonics*, **26**, 573-595.
- Fergusson, C.L., Henderson, R.A., Fanning, C.M., Withnall, I.W., 2007b. Detrital zircon ages in the Neoproterozoic to Ordovician siliciclastic rocks, northeastern Australia: implications for the tectonic history pf the East Gondwana continental margin. *Journal of the Geological Society of London*, **164**, 215-225.
- Fleming, P.D., 1971. Metamorphism of Folding in the Mt Lofty Ranges, South Australia, with Particular Reference to theDawesley–Kanmantoo Area. *Unpubl. Ph.D. Thesis, University of Adelaide*, 316 pp.
- Flöttman. T., James, P., Rogers, J.; and Johnson, T. 1994. Early Palaeozoic foreland thrusting and basin reactivation at the palaeo-Pacific margin of the southeastern Australian Precambrian Craton: a reappraisal of the structural evolution of the southern Adelaide Fold- Thrust Belt. *Tectonophysics* , **234**, 95–116.
- Flöttman. T., James, P., Menpes, R. & 5 others, 1995. Kangaroo Island South Australia: strain and kinematic partitioning during Delamerian basin and platform reactivation. *Australian Journal of Earth Sciences* , **42**, 35-49.
- Flöttman. T., James, P, 1997. Influence of basin architecture on the style of inversion and fold-thrust belt tectonics of the southern Adelaide Fold-Thrust Belt, South Australia. *Journal of Structural Geology* , **19**, 1093-1110.
- Foden, J. D., Elburg, M.A., Turner, S. P.; Sandiford, M., O’Callaghan, J. and Mitchell, S. 2002b. Granite production in the Delamerian Orogen, South Australia. *J. Geol. Soc. Lond.* , **159**, 1–19.

- Foden, J.D., Elburg, M.A., Dougherty-Page, J., Burt, A., 2006. The Timing and Duration of the Delamerian Orogeny: Correlation with the Ross Orogen and Implications for Gondwana Assembly. *The Journal of Geology* , **114**, 189–210.
- Foden, J.D., Sandiford, M., Dougherty-Page, J., Williams, I. 1999. Geochemistry and geochronology of the Rathjen Gneiss: implications for the early tectonic evolution of the Delamerian Orogen. *Aust. J. Earth Sci.* , **46**, 377–389.
- Foden, J.D., Turner, S.P. and Morrison, R.S., 1990. Tectonic implications of Delamerian magmatism in South Australia and western Victoria. In: J.B. Jago and P.S. Moore (Editors), The Evolution of a Late Precambrian-Early Palaeozoic Rift Complex: The Adelaide Geosyncline. *Geol. Soc. Aust., Spec. Publ.*, **16**, 465-482.
- Hayward, N., 1990. Determination of early fold axis orientations in multiply deformed rocks using porphyroblast inclusion trails. *Tectonophysics* , **179**, 353–369.
- Hayward, N., 1992. Microstructural analysis of the classic snowball garnets of southeast Vermont. Evidence for non-rotation. *Journal of Metamorphic Geology* , **10**, 567-587.
- Jung, W.-S., Ree, J.-H., Park, Y., 1999. Non-rotation of garnet porphyroblasts and 3-D inclusion trail data: an example from the Imjingang belt, South Korea. *Tectonophysics* , **307**, 381–395.
- Jenkins, J.F.R., Sandiford, M., 1992. Observations on the tectonic evolution of the southern Adelaide Fold Belt. *Tectonophysics* , **214**, 27-36
- Marshak, S. & Flöttman, T., 1996. Structure and origin of the Fleurieu and Nackara Arcs in the Adelaide fold-thrust belt, South Australia: salient and recess development in the Delamerian Orogen. *Journal of structural geology*, **18**, 891-908.

- Mills, K., 1964. The Structural Geology of an Area East of Springton, South Australia. *Unpubl. Ph.D. Thesis, University of Adelaide*, 497 pp.
- Milnes, A. R.; Compston, W.; and Daily, B. 1977. Pre- to syn-tectonic emplacement of early Palaeozoic granites in southeastern South Australia. *J. Geol. Soc. Aust.* , **24**, 87–106.
- Nishiya, T., Watanabe, T., Yokoyama, k., Kuramoto, Y., 2003. New isotopic constraints on the age of the Halls Reward Metamorphics, North Queensland, Australia: Delamerian metamorphic ages and grenville detritical zircons. *Gondwana Research* , **6**, 241-249
- Offler, R., 1966. The Structure and Metamorphism of the PewseyVale Area, Northeast of Williamstown, South Australia. *Unpubl.Ph.D. Thesis, University of Adelaide*, 128 pp.
- Offler, R., Fleming, P.D., 1968. A synthesis of folding and metamorphism in the Mt. Lofty Ranges, South Australia. *J.Geol. Soc. Aust.*, **15**, 245–266.
- Preiss, W. V., 1987. The Adelaide Geosyncline-late Proterozoic stratigraphy, sedimentation, palaeontology and tectonics. *Bull. geol.Surv. S. Aust.* , **53**, 438.
- Quentin De Gromard, R., 2013. *The significance of E–W structural trends for the Alice Springs Orogeny in the Charters Towers Province, North Queensland. Tectonophysics*, **587**, 168-187.
- Rich B.H., 2006. Permian shortening in the Narragansett Basin of southeastern New England, USA. *Journal of Structural Geology*, **28**, 682 694
- Sandiford, M., Foden, J.D., Zhou, S. and Turner, S.P., 1992. Granite genesis and mechanisms of convergent erogenicbelts with application to the Southern Adelaide Fold Belt. *Trans. R. Sot. Edinburgh: Earth Sci.*, **83**, 83-93.

- Sanislav, I. V., 2010. Porphyroblast rotation and strain localization: Debate settled! Comment. *Geology*, **38(4)**, e204-e204.
- Shah, S. Z., Sayab, M., Aerden, D., & Khan, M. A. (2011). Foliation intersection axes preserved in garnet porphyroblasts from the Swat area, NW Himalaya: A record of successive crustal shortening directions between the Indian plate and Kohistan–Ladakh Island Arc. *Tectonophysics*, **509(1)**, 14-32.
- Steinhardt, C., 1989. Lack of porphyroblast rotation in non-coaxially deformed schist from Petrel Cove, South Australia, and its implication. *Tectonophysics*, **158**, 127-140.
- Thiessen, R.L., Means, W.D., 1980. Classification of fold interference patterns: a reexamination. *Journal of Structural Geology*, **2**, 311-316.
- Turner, S. P. 1996. Petrogenesis of the late-Delamerian gabbroic complex at Black Hill, South Australia: implications for convective thinning of the lithospheric mantle. *Mineral. Petrol.*, **56**, 51–89.
- Turner, S.P., and Foden, J. D., 1996. Petrogenesis of late-Delamerian A-type granites and granophyre, South Australia: magma mingling in the Mannum granite, South Australia. *Mineral. Petrol.*, **56**, 147–169.
- Von der Borch, C. C., 1980. Evolution of the late Proterozoic Adelaide Fold Belt, Australia: comparisons with post-Permian rifts and passive margins. *Tectonophysics*, **70**, 115-134.
- Yeh, M.-W. & Bell, T.H., 2004. Significance of dextral reactivation of an E-W transfer fault in the formation of the Pennsylvania orocline, central Appalachians, *Tectonics*, **23**, TC5009, doi:10.1029/2003TC001593.

Weinberg, R.F., Hasalová, P., Ward, L. & Fanning, C.M., 2013. Interaction between deformation and magma extraction in migmatites: Examples from Kangaroo Island, South Australia. *Geol. Soc. Am Bull.* , **125**, 1282-1300.

-CHAPTER III -

**INCLUSION TRAIL ANALYSIS TECHNIQUES, MULTIPLY
INTERLEAVED GROWTH OF STAUROLITE AND ANDALUSITE,
AND SHIFTING PARTITIONING OF REACTIONS VS
DEFORMATION WITH TIME**

- CHAPTER III-

**INCLUSION TRAIL ANALYSIS TECHNIQUES, MULTIPLY INTERLEAVED GROWTH OF
STAUROLITE AND ANDALUSITE, AND SHIFTING PARTITIONING OF REACTIONS VS
DEFORMATION WITH TIME**

ABSTRACT.....	59
I - INTRODUCTION.....	61
II – GEOLOGICAL SETTING	61
III - DATA.....	62
III – 1. Vertical section striking 140° containing andalusite porphyroblast clusters ...	62
III – 1.1 Spiral-shaped trails	62
a) Core trails.....	63
b) Rim trails abutting D _b cores and S _b trails in general	64
c) Rim trails abutting and continuous with the matrix foliation	65
d) Inclusion trails fully continuous with the matrix foliation	65
III – 1.2 Sigmoidal-shaped trails in staurolite.....	65
III – 1.3 Straight to weakly crenulated trails	66
III – 1.4 The matrix foliation and subsequent bulk shortening.....	66
III – 2. Vertical section (120°) containing andalusite-staurolite cluster	66
III – 2.1 Strongly sigmoidal inclusion trails in staurolite X	67
III – 2.2 Inclusion trails across the rest of the porphyroblast cluster	67
III – 2.3 Inclusion trail orientations across the remainder of the porphyroblast cluster.....	67
III – 3. Mineralogy, Bulk Composition and Pseudosection.....	68

IV - INTERPRETATION	69
IV – 1.Structural setting.....	69
IV – 2.Deformation history.....	70
IV – 3.Timing of porphyroblast growth.....	72
IV – 3.1 Growth during D_b	72
IV – 3.2 Growth during D_c	73
IV – 3.3 Growth during D_d	74
IV – 3.4 Criteria that resolve subtle differences in the timing of different phases .	75
IV – 3.5 Differences in timing between different crystals of 1 phase in a single foliation event	77
IV – 4.The progressive history of development of inclusion trails revealed by staurolite and andalusite.....	78
IV – 5.Growth of staurolite and andalusite in three successive deformations.....	80
V - DISCUSSION.....	81
V – 1.Millipeding during early bulk shortening disguised as spiral trails	81
V – 2.Partitioning variation in time and across different portions of a single sample	82
V – 3.Timing from one porphyroblast encapsulating another	84
V – 4.The implications of multiple phases of growth of both staurolite and andalusite	85
V – 5.Inclusion trail variation in orientation due to porphyroblast rotation?	86
REFERENCES	86

ABSTRACT

Excellent inclusion trails in a staurolite and andalusite-bearing sample preserve 3 main phases of growth of both phases during the early stages of 3 deformation events. Subtle extra periods of growth of both phases occur, being most obvious for andalusite porphyroblasts, which commonly occur as clusters of large crystals that vary from several to tens of degrees in orientation and can encapsulate staurolite grown in an earlier or the same deformation event. All foliations defined by all inclusion trails intersect in a FIA (a foliation intersection axis preserved within porphyroblasts) trending at 25° indicating no change in the direction of horizontal components of bulk shortening while the porphyroblasts grew. Well-preserved microstructural relationships between successive foliations within porphyroblasts allow a detailed analysis of the approaches to inclusion trail description and interpretation that have resulted from 25 years of quantitative FIA based studies. Spiral-shaped inclusion trails in most porphyroblast clusters contain portions of millipede geometries. The latter clinch the dominant role of bulk shortening in porphyroblast growth even in an environment that is overall non coaxial and which results in the same asymmetry later on in each deformation event. Any role for porphyroblast rotation is strongly refuted by differing stages in the development of these bulk-shortening geometries preserved within staurolite and the andalusite that immediately enclosed them as does such variation in adjacent clusters. They strongly suggest that discrepancy in the orientation of inclusion trails in porphyroblast cores is a function of the early effects of bulk shortening driving porphyroblast growth and cannot be used to imply later porphyroblast rotation. Staurolite and andalusite have grown slightly before, after and synchronously, without reacting with each other, during the early stages of 3 separate deformations. This

strongly supports microstructural and more recent metamorphic data that the early stages of bulk shortening start porphyroblast growth; it also indicates that the commencement of the development of a differentiated foliation in the vicinity of a porphyroblast will always stop growth.

Keywords: multiple phases of staurolite growth; synchronous staurolite and andalusite growth; spiral trails from millipeding

I - INTRODUCTION

Porphyroblast inclusion trails provide unparalleled information of the inter-relationships between deformation and metamorphism, yet detailed approaches on how they can be described and interpreted, aside from changes in FIA trend, are rarely documented. This paper redresses that using a sample containing 3 stages of near synchronous staurolite and andalusite growth about a single FIA trend (foliation intersection axes preserved within porphyroblasts) during 3 separate deformations. This detailed approach reveals aspects of the development of partial millipede geometries during progressive bulk shortening that are likely commonplace but have previously gone unrecognized because they lie within overall sigmoidal or spiral inclusion geometries. These millipede portions of the history provide answers to fundamental problems much discussed in recent literature. All aspects of porphyroblast development should be explicable if they contain good inclusion trails and if concepts of the metamorphic/structural processes about how the latter develop are accurate. The numerous periods of growth of both staurolite and andalusite porphyroblastic preserved in this sample provide strong support for concepts developed over the past 30 years plus new aspects regarding the processes involved.

II – GEOLOGICAL SETTING

Sample 43 described herein was collected from a porphyroblastic portion of the Lower Palaeozoic Kanmantoo Group within the Adelaide Fold Belt to the east of Adelaide in South Australia (Fig. 1). This S-shaped oroclinal belt of Upper Proterozoic and Lower Palaeozoic rocks developed with deformation events ranging from a synorogenic granite at 516 Ma and (Foden et al., 1990; Sandiford et al., 1992) through a continuous 495 to 485 Ma spread of ages from U-Pb SHRIMP dating of magmatic rocks derived by anatexis (Weinberg & Hasalova, 2014). The flysch-like sediments of the Kanmantoo

group, which range from anchizonal/unmetamorphosed to migmatitic gneisses, contain 4 generations of foliation at outcrop scale (e.g., Mills, 1964; Offler, 1966; Offler & Fleming, 1968; Fleming, 1971) with at least 5 visible in thin section (Adshead-Bell & Bell, 1999). Sample 43 is a meta-pelite from an outcrop near the contact with the Proterozoic Adelaidean formation where the dominant structural fabric is sub-horizontal. The matrix foliation defining this fabric is composed of aligned elongate shaped biotite, muscovite and quartz. The inclusion trails are mainly defined by quartz, with minor biotite and ilmenite. Sillimanite and chlorite have formed late in the history post staurolite (mms in size) and andalusite (cms in size) growth.

III - DATA

III – 1. Vertical section striking 140° containing andalusite porphyroblast clusters

The thin section shown in Fig. 2 contains 4 large andalusite porphyroblastic masses (*I*, *II*, *III*, *IV*); small portions of the rims of 2 other andalusite masses truncated by the top left and bottom right thin section edge are not described herein. Each of the 4 large andalusite masses consists of a cluster of porphyroblasts that have slightly to significantly different crystallographic orientations (~20°) and grew over a range of times. Figure 2 also contains 4 small staurolite porphyroblasts (*V*, *VI*, *VII*, *VIII*) portions of which also grew over a range of times.

III – 1.1 Spiral-shaped trails

The large andalusite porphyroblast clusters *I* through *IV* and staurolite *V* in Figs 2 and 3a to 3e contain spiral-shaped inclusion trails that are either truncated by or merge with the gently southeast pitching schistosity S_c in the matrix (coloured yellow). The spiral shaped inclusion trails are partly defined by a steeply but variably pitching differentiated crenulation cleavage S_b (coloured red) at stage 3 to 4 of development (Bell & Rubenach, 1983) that curves overall clockwise towards a more gentle pitch.

The crenulated cleavage S_a (coloured green) is preserved relatively unaffected in the cores of andalusite clusters **I** (Fig. 3a) and **II** (Fig. 3b) and staurolite porphyroblast **V** (Fig. 3e).

a) *Core trails*

In **I**, S_a is strongly truncated by S_b defining a distinct microstructural core that formed post S_a and since S_a is curved locally within it due to the development of S_b , most likely formed early during D_b (Figs 2 & 3a). This occurs to a lesser degree in **V** (Fig. 3e). In **II**, differentiation associated with stage 3 of S_b crenulation cleavage development occurs on both sides of an irregularly shaped quartz rich core region marked b. S_a within the core is not truncated as rotates into the zone of S_b differentiation on the right side but it is truncated by S_b on the far left side and within the strain shadow is continuous preserves S_a curving continuously into S_b on the right of the cluster centre where the trails are straight and appears to do something similar on the left (Figs 2 and 3b). Superficially, there is no portion defining a certain core against which S_b has intensified. However, the detail shown in Fig. 3b reveals that the bulk of the rectangular protrusion on the left of the crystal of andalusite that overgrows the core contains S_a in a similar orientation to that in the central portion. Only the differentiated material above and below this rectangular protrusion of the core contains steeply pitching S_b with a generally finer grain size and containing less quartz than in S_a across the bulk of the core. Thus S_b on the left locally intensifies against the core crystal suggesting that it developed after that portion of the andalusite cluster grew. Furthermore, variation in S_a due to the effects of D_b across the core suggest that the core grew early syn D_b in this portion of the rock. It is likely that the left arm of the core did not protrude as far to the left in the portion or rock that lay above and below this thin section, resulting in the intimate wrapping of S_b relative to S_a around the left arm.

The following details have significance for the interpretation: -

1. In **I** a single andalusite crystal encompasses all S_a preserved in the distinctly truncated core but incorporates some S_b on its right side (Fig. 3a).
2. In **II**, a single andalusite crystal encompasses most of the S_a that has not been rotated into differentiated S_b . (Fig. 3b).
3. The centres of porphyroblast clusters **III** (Fig. 3c) and **IV** (Fig. 3d) contain evidence for thinner seams of the same differentiated crenulation cleavage present in their rims that is not present in the cores of **I** and **II**.
4. For **III** and **IV** (Figs 3c & 3d), a single andalusite crystal reaches laterally across the centre from just into differentiated S_b on one side to the opposite rim while another differently oriented crystal incorporates most of the opposite rim. The bottom left corner of **II** appears to overgrow a little differentiated S_b (Fig. 3b) except that the bulk of differentiated S_b on both sides is overgrown by other andalusite crystals. This does not occur for **I** (Fig. 3a).
5. For **I** (Fig. 3a) and **V** (Fig. 3e), S_b against the microstructural core is sub-vertically pitching. This is not the case for **II**, but above and below the protruding left arm of the core crystal, S_b is sub-vertical (Fig. 3b).

b) Rim trails abutting D_b cores and S_b trails in general

Generally, steeply pitching S_b trails curve smoothly clockwise towards the horizontal in **I** through **VII** (Figs 3a to 3g). S_b trails curve past the horizontal into differentiated S_c on the bottom left edge of **I** (Fig. 3a), **II** (Fig. 3b) and **VII** (Fig. 3g). They are locally truncated by the sub-horizontal to gently SE pitching matrix foliation S_c on the upper rims of **I**, **III**, **IV** (Figs 3a, 3c & 3d) and lower rim of **I**, **II**, **III**, **IV** and **VI** (Figs 3a, 3b, 3c & 3f). Superficially, they can appear to be continuous with the matrix foliation S_c . However, detailed examination reveals that all S_c foliations preserved in porphyroblast

rims truncate S_b or, in the case of the upper and lower rims of **VII** (Fig. 3g), form a differentiated crenulation cleavage that effectively truncates S_b . Generally, S_c forming in the strain shadow of a porphyroblast overprints crenulated relics of S_b .

c) Rim trails abutting and continuous with the matrix foliation

The lower left extremity of **I** (Fig. 3a), the lower left rim of **II** (Fig. 3b) and the lower rim of **VII** (Fig. 3g) locally contain S_c within the edge of the porphyroblast or porphyroblast cluster. S_b , rotated and differentiated by D_c is preserved within S_c in the upper rim of **VII** (Fig. 3g).

d) Inclusion trails fully continuous with the matrix foliation

The only inclusion trails that are entirely continuous with the matrix foliation are those where a porphyroblast has overgrown fully developed S_c such as the staurolite porphyroblast **VIII** (Fig. 3h) and the similarly sized andalusite crystal directly above, which at high magnification is separate from the bottom of cluster **III** (Figs 3c & 3h).

III – 1.2 Sigmoidal-shaped trails in staurolite

Staurolite porphyroblasts **VI** and **VII** contain only sigmoidal-shaped inclusion trails that pitch moderately NW in the central portion of these 2 crystals in Figs 2, 3f & 3g. Where the trails are strongly rotated towards the sub-horizontal, less inclusions are present and the amount of encapsulating staurolite is greater because of the differentiation that concentrated phyllosilicates along S_c before rim growth occurred. The gently dipping foliation in the upper rim of **VI** (Fig. 3f) and upper and lower rims of **VII** (Fig. 3g) is continuous with the latter foliation. The density of inclusion trails encapsulating the NW pitching foliation in the porphyroblast centres, as well as the amount of staurolite that encapsulates them is the same as for S_b abutting the core in **V** (Fig. 3e).

III – 1.3 Straight to weakly crenulated trails

Staurolite *VIII* and the andalusite crystal lying immediately above (Fig. 3h) at the bottom of *III* only contain S_c . S_c in both is weakly crenulated about a steeply pitching axial plane direction (S_d) whose deformation affects are more visible to the right and left of these two crystals. The rotational effects of this crenulation event are readily visible on the left side of *IV* where the steep character of the axial plane is apparent in the matrix above *III* (Fig. 2).

III – 1.4 The matrix foliation and subsequent bulk shortening

The matrix foliation, S_c , away from the strain shadow protection provided by *I* through *VII*, such as in the lower left and top right of Fig. 2 is pitching to the SE at around 40°. Between the porphyroblasts where the strain shadow protection provided by each large crystal is greatest, S_c is gently dipping with sub-horizontal dips preserved above and below the approximate centres of clusters *I* through *IV* and porphyroblasts *V* through *VII*. These relationships and the crenulations mentioned above would result from sub-horizontal bulk shortening during D_d . Measuring the average pitch of S_c away from porphyroblasts in 12 differently oriented vertical thin sections and combining them on a stereo produced an orientation for S_c of 20°SE/60°. Anastomosing of S_c around the porphyroblasts and the weak effects of D_d generated the local 40° pitch in this thin section.

III – 2. Vertical section (120°) containing andalusite-staurolite cluster

This section, cut adjacent to but ~ 4cms at its maximum distance from that described above striking at 140°, contains 3 staurolite porphyroblasts that are included within a cluster (*IX*) of 3 differently oriented andalusite crystals (Fig. 4a,b). Staurolite porphyroblast (*X* Figs 4a,b and 5a) and the andalusite cluster (Fig. 4a,b) each contain sigmoidal shaped trails that in combination define a spiral shape.

III – 2.1 Strongly sigmoidal inclusion trails in staurolite X

Staurolite *X* (Fig. 5a) contains a core with a strongly developed stage 3 to locally stage 4 of differentiated crenulation cleavage (S_b , Bell & Rubenach, 1983) abutting its left side (and to a lesser extent its right side). The foliation in the core, S_a , which is truncated on the lower left side of the core by S_b , coarsened into the latter, within the strain shadows above and below as large blocky quartz, before the growth of staurolite across the rim took place. S_a within the core is defined by fewer and smaller opaques than S_b in the rim to the left and right.

III – 2.2 Inclusion trails across the rest of the porphyroblast cluster

The character of the S_b foliation defined by the inclusion trails in the other staurolite porphyroblasts (Figs 5b & 5c) as well as in the cluster of surrounding andalusite (Fig. 4a,b) is identical to that within the left and right rims of *X* (Fig. 5a). It is also identical to the steeply pitching fully differentiated portions of S_b within the left and right rims of *I* through *IV* in Figs 2, 3a, 3b, 3c & 3d. A significant difference between Figs 2 and 4 that is interpreted below is that no relics of S_a are present anywhere outside staurolite *X* within andalusite in the rest of the porphyroblast cluster in Fig. 4. Indeed, one could argue that S_b is effectively at stage 6 of crenulation cleavage development because no relics of S_a are visible anywhere across a large width of this foliation (Bell & Rubenach, 1983).

III – 2.3 Inclusion trail orientations across the remainder of the porphyroblast cluster

The inclusion trails defining S_b exit from staurolite *X* into the surrounding andalusite (Fig. 4) with the same orientation they have in the rim of the former except for a very slight clockwise deflection on the lower left of centre (Fig. 5a). Outside staurolite *X* in Fig. 5a, S_b inclusion trails have an overall clockwise sigmoidal shape but significant deflections take place within staurolite porphyroblasts *XI* and *XII* and the andalusite

that surrounds them. Details in these deflections that are significant for interpretation are as follows: -

1. The inclusion trails in **XI** spread outwards laterally to either side of sub-vertical towards the bottom of the porphyroblast (Fig. 5b) into half a millipede shape indicative of sub-vertical bulk shortening (Bell, 1981).
2. The inclusion trails in **XII** are spread similarly but less towards the bottom (Fig. 5c) than those in **XI**, but with that spread increasing after they exit (Fig. 4).
3. Locally, the inclusion trails in andalusite immediately adjacent to the bottom left of staurolite **XI** curve sharply clockwise from vertical as they exit the staurolite (Fig. 5b).
4. The inclusion trails in andalusite spread towards the base of the photo to the left and to the right of **XI** and **XII** to a greater degree than the half millipede-like widening visible in either staurolite porphyroblast (Figs 4, 5b & 5c).
5. Below **XII** the inclusion trails in andalusite begin to curve clockwise to match the curvature above **XI** in Fig. 4.
6. The inclusion trails in andalusite above **XI** remain vertical until they reach the right side of the protruding corner of **X** where they begin to curve smoothly clockwise (Fig. 4).

III – 3. Mineralogy, Bulk Composition and Pseudosection

Using the 8 most differently oriented vertical thin sections made, this sample modally contains 1.38% staurolite and 7.21% andalusite porphyroblasts. Using a vertical section striking sub-parallel to the FIA at 20° to limit any heterogeneous effects of differentiation and cleavage seam development during D_b and not allowing for inclusion trails within these 2 porphyroblastic phases the matrix consists of 31.95% quartz, 4.68% ilmenite, 36% biotite and 17.55% muscovite. Local patches of coarse-grained deformed vein quartz occur adjacent to andalusite clusters, and some contain late fibrolite. Coarse

retrograde chlorite (0.86%) occurs locally. The XRF determined bulk composition of this sample is Al₂O₃ 18.794, SiO₂ 59.505, CaO 1.679, MgO 3.819, Fe₂O₃ 7.777, K₂O 3.557 Na₂O 2.248, MnO 0.09, TiO₂ 0.762. A pseudosection constructed in the MnNCKFMASH system is shown in Fig. 6 and reveals an extremely tight region of PT space where staurolite and andalusite coexist between 3.8 and 4.1 kbar and 560 and 575°C.

IV - INTERPRETATION

IV – 1. Structural setting

The porphyroblasts in this sample all contain a FIA trending at 25° which is the 4th of 5 FIAs that formed in this region (Fay & Bell, 2015 unpublished data). The deformation history interpreted below for this limited portion of the total FIA history will apply to other samples containing this FIA trend, although less, or locally even more, foliations could be developed about this particular trend in some samples. For example, in Vermont, 5 FIA trends are each defined by between 2 and 7 foliations from sample to sample (Ham & Bell, 2004; Bell & Newman, 2006). The number of foliations defining a FIA, and different FIAs in proximal samples, results from them recording different histories because deformation routinely partitions at all scales (e.g., Sanislav & Bell, 2011; Bell et al., 2013). Some of the many deformations that affected the Kanmantoo region and produced the three earlier formed FIAs will have impacted on the development of the oldest foliation visible and labelled S_a in Figs 2 to 5 that pre-dates all andalusite and staurolite growth therein. Indeed, because S_a was gently dipping prior to the commencement of the growth of these phases in this sample (see below), this foliation could have formed before or during the development of any of the preceding three FIAs that developed in this region (e.g., Bell & Sanislav, 2011). All that is needed for this to have occurred is that no deformation partitioned through this location on the

scale of a porphyroblast during any of the intervening deformation history associated with development of the those FIA sets (e.g., Sanislav & Bell, 2011; Bell et al., 2013). The importance of this phenomenon will be emphasized below as it is vital for understanding porphyroblast growth in general and how the growth of staurolite and andalusite started and stopped repeatedly during three deformation events herein.

IV – 2. Deformation history

The core of the andalusite clusters *I* and *II* and staurolite *V* in Figs 2, 3a, 3b & 3e and *X* in Figs 4 & 5a preserve the oldest foliation (S_a) present in this sample where it has been least affected by the effects of development of the next deformation. The inclusion trails defining S_a pitch gently to moderately SE curving slightly concave downwards in Fig. 2 on the left and right extremities of the lower portion of the core but clockwise on both sides of *II*, *V* (Figs 2, 3b & 3e) and *X* (Figs 4 & 5a). This suggests bulk shortening was sub-horizontal during D_b and that its effects were initially near coaxial in the location where *I* grew (compare it with figs 15 & 6 in Bell & Bruce 2006 and 2007 respectively). S_a is fully truncated by differentiated S_b outside the microstructural core in *I* but not in *II* (Figs 2, 3a & 3b). S_a is truncated partially to fully outside the core of *V* (Figs 2 & 3e) and locally in *X* (Figs 4 & 5a). Finally, relics of S_a preserved within andalusites *III* and *IV* also pitch SE and curve clockwise (looking NE) into differentiated S_b (Figs 2, 3c & 3d).

S_b ranges from differentiated crenulation cleavage seams containing relics of Q-domains preserving crenulated S_a in andalusites *III* and *IV* (Figs 2, 3c & 3d) to fully differentiated and containing no relics of S_a in andalusite in Fig. 4. S_b pitches sub-vertically against the left and right extremities of D_b cores in *I*, *II* and *V* in Figs 2, 3a, 3b & 3e and *X* in Figs 4 & 5a strongly supporting the interpretation that it formed during bulk horizontal shortening.

S_c , the dominant matrix foliation, ranges from sub-horizontally pitching where protected in strain shadow regions between porphyroblasts to moderately SE pitching. In the sample it is oriented mesoscopically in 3D at $20^\circ\text{SE}/60^\circ$. S_c is intensely differentiated against gently pitching rims of the andalusite clusters (Figs 2 & 4) and staurolites *V*, *VI*, *VIII* in (Fig. 2). Bulk shortening during D_c was sub-vertical and caused S_b to deflect to both the WNW and ESE during the coaxial early stages of this deformation. This is most apparent within staurolites *XI* and *XII* in Figs 4, 5b & 5c, but has also occurred within andalusites *III* and *IV* in Figs 2, 3c & 3d; these features will be interpreted in detail below (in the section on growth during D_c). When deformation during D_c intensified it went non-coaxial top to the SE.

Open crenulations of S_c in the matrix have steep axial planes labelled S_d in Figs 2 & 4 that pitch steeply within 15° to either side of the vertical. These crenulations were significant for further porphyroblast growth and their FIA within porphyroblast rims, which trends at 25° , is the same as for the earlier formed foliations. They are particularly well developed against the left rim of staurolite *VIII* and right rim of the andalusite crystal lying immediately above on the bottom of porphyroblast cluster *III* where they show no overall asymmetry (Fig. 3h). However, they tend to rotate S_c clockwise looking NE and cause some weak local coarse differentiation against the lower right rim of *III* (Figs 2 & 3c), left rim of *VI* (Figs 2 & 3d) and in the matrix to the right of *IV* below *III* (Fig. 2) suggesting that the deformation became a little non-coaxial clockwise as it intensified. This would have given the matrix foliation its average 20° dip to the SE.

Consequently, within this sample each deformation post D_a began coaxial and went non coaxial clockwise with time. Looking NE, shearing was up to the WNW on S_b , top to the ESE on S_c and up to the WNW on S_d .

IV – 3. Timing of porphyroblast growth

Three main periods of porphyroblast growth, which occurred during the three deformations D_b , D_c and D_d mentioned above, are visible in the photograph of the 140° striking vertical section of this sample shown in Fig. 2. They are also visible in in Fig. 4 from the 120° striking vertical section although D_d growth is less obvious and only most certain in the right side of the small patch of very poikiloblastic andalusite in the top right corner of the cluster. Some subtle timing differences for different crystals in the porphyroblast clusters are also distinguishable in Figs 2 to 5 within both D_b and D_c that are described separately.

IV – 3.1 Growth during D_b

The first phase of growth, which occurred during D_b , is preserved in the cores of andalusite clusters *I* (Figs 2, 3a, 8) and *II* (Figs 2 & 3b) and staurolites *V* (Figs 2 & 3e) and *X* (Figs 4, 5a & 9). Initially, cluster *II* appeared to not have the key timing criteria of S_b intensified against and/or wrapping around distinctive core margins. However, recognition

1. that an arm of the differently oriented andalusite in the cluster centre core extends to the bottom left preserving S_a in a similar orientation to that in the core (Figs 2 & 3b)
 2. that this latter portion of S_a is undifferentiated by the effects of D_b
 3. that differentiation during D_b intensified above and below and on the left edge of this latter portion of S_a , meant that different aspects of the key timing criteria of S_b intensified against a core are present that indicate that early D_b growth occurred.
- Although D_b growth entrapped coarse-grained quartz within S_a inclusion trails in andalusite clusters *I* and *II* (Figs 2, 3a & 3b; c.f. 8a & 8b for *I*) with overall much less and finer-grained quartz within S_b trails trapped subsequently to either side, the equivalent cores in staurolites *V* (Figs 2 & 3e) and *X* (Figs 4, 5a; c.f. 9b1 & 9b2) show

lesser changes relative to their rims. The main change in the latter mineral phase is, that away from the blocky strain shadow quartz on the core boundary, longer slimmer quartz grains define S_b in the rim than S_a in the core. Growth of staurolite appears to have required the higher phyllosilicate content of more differentiated layers from D_a . The S_a inclusion trails preserved in all D_b grown cores in Figs 2, 3a, 3b, 4, 5a, 8 & 9 are gently to moderately SE pitching; they curve clockwise on the left and right edges of each core except the left side of that in *I* where they curve anticlockwise suggesting coaxial deformation during the earliest stages of D_b (Figs 2, 3a & 8a). S_b at stage 4 of crenulation cleavage development (Bell & Rubenach, 1983) truncates the core on both sides of *I* (Figs 3a & 8b) and the right side of *V* in Figs 2 & 3e. S_b ranges from stage 3 of crenulation cleavage development within which S_a is continuous across zones of S_b differentiation (right side of *II* in Figs 2 & 3b) to partially truncated (top left side of *II* in Figs 2 & 3b) to almost stage 4 (both sides of core of *V* in Figs 2 & 3e) and the left side of *X* (Figs 4, 5a & 9c2) to fully truncated stage 4 in *I* in Figs 2, 3a & 8b. Where S_b has developed to stage 4 and truncates S_a trails against the core it is steeply pitching suggesting that it formed sub-vertically (e.g., Hayward, 1992; Bell & Sapkota, 2012).

IV – 3.2 Growth during D_c

The second phase of growth, which occurred during D_c , overgrew differentiated S_b at stages ranging from 3 and 4 (Fig. 2) to 6 (Fig. 4) of crenulation cleavage development in the andalusite clusters and all staurolites apart from *VIII*, which grew in D_d (see below). The initial effects of D_c on S_b were coaxial with the latter being rotated both clockwise and anticlockwise (Fig. 8c). This millipeding effect is very apparent in Figs 4 & 5 where sub-vertical S_b in staurolites *XI* and *XII* (Figs 9c1 & 9c2) spreads apart to either side of the vertical towards their lower boundaries in the manner of the longitudinal half of a millipede geometry (Bell, 1981). This millipeding was further

developed in S_b surrounding them immediately prior to growth of the andalusite that then occurred to either side of **XI** and **XII** (Figs 4, 5 & 9c3). Without the presence of staurolite the latter geometry would not have developed so obviously in the andalusite. S_b was locally shortened significantly vertically with a clockwise asymmetry, against the left side of the base of **XI** where it exits the latter crystal, before andalusite grew (Fig. 5b). The resulting inclusion trail geometry in andalusite in these figures is quite similar to that lying between **I** and **III** within the right and left rims of these two clusters respectively (Figs 2, 8c & 8d). A horizontal traverse across the centre of **IV** in Figs 2 & 3d preserves a less developed but similar geometry that would be just regarded as part of the spiral except for the above described relationships. Thus in **III** and **IV**, anticlockwise rotation of S_b from sub-vertical to pitches of 56° and 62° SE respectively has taken place near their centres due to the early millipede like coaxial effects of D_c . The preservation of sub-vertical S_b in the D_c strain shadow against the core of **I** confirms this interpretation for **III** (compare Figs 8c through 8f). The anticlockwise anastomosing of S_b around the lower left corner of the core of **I** (Fig. 8e) was exaggerated (Figs 8f & 8g) as crenulation of S_b developed just after the commencement of D_c . Thus, vertical bulk shortening at the commencement of D_c resulted in early millipeding of S_b , anticlockwise rotation of S_b and finally the strongly clockwise non-coaxial deformation that eventually formed the intense matrix S_c (Fig. 8h). This changed S_b from the sigmoidal shape to either side of the core **I** to a more spiral shape within the core of **III** and **IV** (Fig. 2) and the centre to lower right half of the andalusite cluster in Figs 4, 9c1, 9c2 & 9c3.

IV – 3.3 Growth during D_d

The third phase of growth during D_d overgrew differentiated S_c in staurolite **VIII** (Fig 3h) and the bottom left of **VII**. This also occurred in andalusite (Fig. 9j) adjacent to the

bottom of cluster **III** (immediately above **VIII** in Fig. 3h; see also Fig. 8j), the bottom left of **I** (Figs 2, 3a, 8i & 8j), the bottom left of **II** (Figs 2 & 3b) and perhaps just along the top of **III** in Fig. 2. Only very minor growth during D_d is visible in Figs 4, 9d2 & 9d3 in the small very poikiloblastic but differently oriented crystal to the right of the cluster centre. Growth over portions where S_c was partially developed and the relic crenulation hinges in S_b are still partially preserved occurred near the upper rims of **I** and **VII**. As mentioned above, D_d was a relatively weak event that formed more open crenulations with steeply dipping axial planes (Fig. 7) that began coaxially and went slightly non-coaxially clockwise with time giving the shallowly dipping S_c its 20° to the SE tilt.

IV – 3.4 Criteria that resolve subtle differences in the timing of different phases

The heterogeneous partitioning of deformation with time through a rock mass, combined with which developing crenulation hinges microfracture and grow porphyroblasts (Bell & Hayward, 1991; Bell & Bruce, 2007), means that timing different phases is best accomplished within a cluster developing in one event. Such a cluster will be affected by the same bulk amount of relatively low strain inducing progressive bulk shortening throughout the event in which the crystals being compared grew. This dramatically reduces the pervasive problem of heterogeneity across and along foliations that normally prevent most microstructural relationships being used to closely examine and interpret subtle differences in relative timing within the one deformation. The extent of this problem is apparent from a comparison of inclusion trails preserved by growth during D_c over S_b between the 5 andalusite clusters in Figs 2 & 4. The 4 clusters in Fig. 2 lie in one thin section and the 5th lies less than 3cms away in another (Fig. 4) as the two sections were cut using adjacent vertical blocks through the same horizontal slab. Bulk sub-vertical shortening appears to have produced

millipede effects, even if they look like spirals, in some of the clusters in Fig. 2 as shown in Figs 8c & 8d. This interpretation is strongly supported by the andalusite cluster in Fig. 4, which encloses 3 staurolite porphyroblasts. Two of the staurolites record distinct half millipedes forming during D_c (Figs 9c1 & 9c2) that were further developed in the surrounding andalusite that overgrew and enclosed them slightly later on in the same event (Fig. 9c3). S_b is effectively at stage 6 of crenulation cleavage development across the cluster in Fig. 4 but ranges from stage 3 to 4 in the clusters in Fig. 2. Furthermore, for growth during D_b , S_a varies in pitch from 20° to 25° to 45° SE in the four D_b cores *X*, *III*, and *V*, respectively providing no indication of relative timing of staurolite vs andalusite from the amount of rotation. Similarly the scale of partitioning provides no indication except perhaps for the same phase. For example, consider the smaller staurolite cores in *V* and *X* vs the larger andalusite cores in Figs 2 & 4. The former most likely resulted from the crenulations developing at smaller wavelengths within finer grained more differentiated phyllosilicate rich layers where staurolite preferentially nucleated. Such more phyllosilicate rich layers would likely have formed from the effects of deformation partitioning that predated or occurred during D_a .

Staurolite growth occurred before andalusite growth during D_c in Fig. 4 because the half millipedes are less and differentially developed in the former than the latter phase (as shown in Figs 9c1, 9c2, & 9c3). Furthermore, S_b was locally strongly rotated clockwise against the lower left rim of *XI* before andalusite grew (Fig. 5b). This supports changes in FIA trend that match dated successions of one porphyroblastic phase enclosed by another that have always revealed the former grew earlier (e.g. Ali, 2009 and many others since). The difference in timing is slight but of interest relative to the pseudosection from this sample (see below). No relative timing of these two phases

during D_c is available from Fig. 2 as that section does not contain them together in a cluster. No conclusive relative timing of these two phases is available for their growth during D_b . Keeping in mind the problems of deformation heterogeneity across foliations, there is a hint that the andalusite core in *I* may have grown slightly before the staurolite core in *V* as it preserves more coaxial strain in its rim, but many more examples of this would have to be seen from other thin sections.

Staurolite and andalusite grew adjacent to one another between clusters *III* and *IV* over well-developed S_c . They can be directly compared because growth took place during D_d when they were in the strain shadow created by those two clusters and the foliation they enclose would have been affected by the same amount of bulk horizontal shortening when they were growing. No difference is visible (Fig. 3h).

In conclusion the possibility exists of andalusite growing slightly before staurolite in D_b (Fig. 2), staurolite definitely grew slightly before andalusite in Fig. 4 in D_c (Figs 9c1 to 9c3) and they appear to have grown at essentially the same time in D_d . What can be stated with certainty is that growth of staurolite and andalusite was almost synchronous for each of the three events.

IV – 3.5 Differences in timing between different crystals of 1 phase in a single foliation event

The control of deformation partitioning on where porphyroblast growth begins and ceases has been documented many times microstructurally for ~30 years. Recently it has also been well documented metamorphically (e.g., Sanislav & Bell, 2011; Bell et al., 2013). The cluster of andalusite crystals in *I* provides another perspective on this phenomenon with differentiated S_b on the both sides of where the core grew being overgrown by different crystals to that in the core (Figs 2 & 3a). Yet a portion of that on the right side was still overgrown by the same crystal as in the core. The other feature of

this cluster is the change in inclusion trail geometries between the two crystals on the left side of the total cluster. The foliation is continuous from one crystal to the other across the gap between them where they are the least poikiloblastic. Coarse strain shadow quartz lies in the rest. In the third dimension the portion to the left may extend from the core of another proximal cluster. Alternatively, it is part of cluster *I* and grew slightly after the andalusite crystal to the right (compare Figs 8g & 8h). Cluster *IV* preserves a greater variation in the timing of growth within D_c with the crystal that incorporates the centre growing across and from the centre just after the anticlockwise rotation of S_b towards the right. The crystal lying below and the top and bottom of that on the left grew slightly later after CW rotation of S_b dominated.

IV – 4. The progressive history of development of inclusion trails revealed by staurolite and andalusite

Figures 8 & 9 show models for the progressive development of the inclusion trails preserved in the porphyroblasts in Figs 2 through 5. They involve variation in the impact of partitioning for the same as well as successive deformations at different scales on the deformation and metamorphic events preserved in these proximal but different portions of this sample. Before porphyroblast growth began, a gently dipping foliation S_a was produced during sub-vertical bulk shortening event D_a (Fig. 9a). S_a began to be crenulated at a range of scales by the effects of sub-horizontal bulk shortening event D_b . This range of scales is apparent from a comparison of the small staurolite core in porphyroblast *X* in Figs 4, 9b1 & 9b2, the large andalusite core in porphyroblast *I* in Figs 2 & 8a, and the similar but larger geometry of the S_a/S_b trails in the centre of andalusite porphyroblast *IV* in (Fig. 2). The history of D_b staurolite core growth is shown in progressive detail in Figs 9b1 & 9b2 for the staurolite porphyroblast *X* from Figs 4 & 5a and the history for andalusite porphyroblast *I* in Figs 2 & 3a is similar as

shown in Figs 8a & 8b. Differentiation occurred with the local development of S_b best seen against the right margin of the staurolite and andalusite cores just mentioned. Elsewhere, the effects of D_b were more varied as S_b developed with decrenulation and reactivation of S_a occurring as it was rotated towards S_b .

Figure 8a shows the location where the andalusite porphyroblast *I* in Fig. 2 grew and *III* eventually grew. The history is similar to the location where staurolite *X* growth took place in Figs 4 and 9b1 except that the scale of partitioning of differentiation during D_b was much coarser. Of course, once a porphyroblast does nucleate, its competency relative to the matrix localizes strain development against its margins (Bell & Bruce, 2007). Truncational S_b cleavage then developed (Fig. 8b).

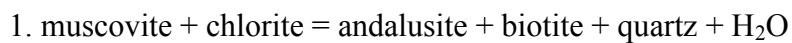
Figures 9c1 to 9c3 show the growth of staurolite early during the development of D_c . The early stages of any deformation are commonly very coaxial (Bell & Newman, 2006) and this results in the initial development of millipede geometries that locally lead to microfracture (Bell & Hayward, 1991) and thus porphyroblast nucleation and growth (e.g., fig. 15 in Bell & Bruce, 2006). Staurolite nucleated on variably weakly crenulated and millipeded S_b early during D_c in porphyroblasts *XI* and *XII* as well as began to overgrow the rims against the core of *X* in Figs 9c1 & 9c2. It is noteworthy that the inclusion trails in staurolite *X* are slightly more rotated CW than those in the andalusite below but less than in the andalusite above in Fig. 4. This suggests that deformation partitioned a little more intensely against the upper staurolite rim, possibly because a strain shadow due to the presence of staurolites *XI* and *XII* protected the lower rim (Fig. 9c2). This was followed by the growth of the bulk of the cluster of andalusite porphyroblasts over all 3 staurolites (Fig. 9c3).

The finer scale of partitioning in staurolite in Figs 2 & 4 could suggest it nucleated after andalusite but deformation may simply have started in the location

where staurolite eventually grew before where andalusite *I* grew. Alternatively, staurolite grew in more micaceous portions that developed before or during D_a time and they would have crenulated at a finer scale earlier in the same deformation event because of the effect of layer thickness on fold wavelength (Biot, 1957, 1965; Ramberg, 1963).

IV – 5. Growth of staurolite and andalusite in three successive deformations

Staurolite and andalusite grew in close proximity to one another with no evidence of reaction between them within each of three successive deformations. A pseudosection of this sample (Fig. 6) shows that staurolite and andalusite coexist over a very small portion of PT space between 3.8 and 4.1 kbar and 560 and 575°C. Each of these phases could grow without involving the other from the following reactions.



However, only muscovite and biotite are present in the matrix foliation and only the latter is preserved within inclusion trails in andalusite. The only chlorite present postdates and locally replaces biotite. Chlorite may have been present before D_b growth. However, the lack of this phase as inclusions defining successive foliations within any of the three periods of growth of andalusite suggests that it was gone before D_c and D_d occurred and possibly all consumed before D_b growth began. This is supported by the pseudosection in Fig. 6 where chlorite does not exist in the field where staurolite and andalusite coexist. It could have been present prior to the D_b period of growth of these two phases but not again until late D_d where some alteration of biotite to chlorite appears to have occurred suggesting a slight P increase or T drop. The lack of chlorite and the late alteration of biotite to chlorite suggests that ionic reactions involving

components of matrix biotite were involved in the growth of both staurolite and andalusite.

V - DISCUSSION

V – 1. Millipeding during early bulk shortening disguised as spiral trails

The general role of coaxial bulk shortening during the early stages of newly commencing deformations first became apparent in the control of crenulation hinges on sites of porphyroblast nucleation and growth (Bell et al., 1986). This microstructural observation became more compelling when spiral-shaped inclusion trails resulting from overprinting near orthogonal crenulations were documented (Bell & Johnson, 1989). Evidence for strong coaxiality on the bulk scale in the portions of the crust where porphyroblasts were growing was recognized much later when inclusion trail asymmetry was analysed relative to multiple successions of different FIA trends in orogens the world over (e.g., Ham & Bell, 2004). This analysis of inclusion trail asymmetry variation in the context of successive FIA sets revealed spiral-shaped trails, which previously suggested massive lateral displacements, can develop in tectonic environments that macroscopically are relatively coaxial (e.g., Bell & Newman, 2006). In fact, one asymmetry of inclusion trails for a transition from gently to steeply dipping foliations or vice versa for all samples containing a particular FIA is rare. It has only been recorded by 3 out of more than 25 researchers and then only for changes from steeply to gently dipping foliations for one of several FIA sets measured in each region. Each example provided precise timing on the development of a large-scale nappe that macroscopically overturned bedding within a lengthy history of deformation events (Yeh, 2001; Rich, 2005; Bruce, 2007).

Sample 43 reveals millipede geometries hidden with an overall spiral inclusion trail geometry. These are not the cut effect millipedes or full coaxial millipedes within a

long history of successive foliation development such as those described by Bell & Johnson (1989). Rather, their development helps define the spiral inclusion shape. In the case of Fig. 4, the millipedes (or more accurately half millipedes) are undeniable because they developed separately and differently, prior to or, during the growth of staurolites *XI* and *XII* (Figs 8c1 & 8c2). A larger scale more exaggerated millipede shape developed in S_b outside those porphyroblasts before being overgrown by andalusite slightly later in the same deformation event (Fig. 8c3). The recognition of a role for millipede development in Fig. 2 arose from the foliation S_b being sub-vertical against the right and left rims of the D_b grown core (Figs 9a & 9b) but swinging clockwise away from that orientation in the matrix below and anticlockwise to the right (Fig. 9c). It was then overgrown by andalusite in clusters *I* and *III* during D_c . Understanding this allows one to see similar geometric effects to those in *III* within cluster *IV*. In other words the coaxiality of the early stages of deformation during D_c is well preserved in this sample in spite of the development of spiral shaped inclusion trails in *III*. This is probably a common feature of inclusion trails that has gone unremarked because of its subtle nature. It is important, as it confirms the variation in inclusion trail asymmetries seen across fold limbs and along and across orogens that signify deformation tends to be close to coaxial overall in orogen cores where porphyroblasts are growing (e.g., Ham & Bell, 2004; Bell & Newman, 2006; Bell & Sapkota, 2012).

V – 2.Partitioning variation in time and across different portions of a single sample

Within a single FIA set, the effects of different deformation events that form *steeply* dipping axial planes are only visible if earlier formed *steeply* dipping foliation has been rotated away from the vertical by an intervening event that produced structures with gently dipping axial planes (e.g., Bell & Hayward, 1991). Where no such rotation

occurs, the earlier formed sub-vertical foliation and any associated fold structures are simply intensified by the next deformation forming with a steeply dipping axial plane. This applies independent of FIA set for different deformations forming *gently* dipping foliations (e.g., Bell et al., 2013) because they all form with the same sub-horizontal orientation. Therefore, for a single FIA set, successive deformations switching from sub-horizontal to sub-vertical bulk shortening or vice versa, will orthogonally shorten any previously newly developed foliation. This is not necessarily the case for a sub-vertical foliation if the subsequently developing FIA trend shifts significantly because it can reactivate and undergo shearing rather than crenulate during vertical bulk shortening and no porphyroblasts will grow (section 6.9.1 in Bell et al., 2013). However, for a single FIA succession of foliations as is the case in sample 43, bulk shortening in either direction leads to the development of millipedes and coaxial crenulations that only go non-coaxial as the deformation intensifies. High strains leading to the development of differentiated crenulation cleavages are only possible through the partitioned development of non-coaxial strain, but the microfractures required for the growth of porphyroblasts form during the coaxial early stages. They cease to develop as non-coaxial strain intensifies through geometric softening and strain softening associated with differentiated cleavage development (e.g., Bell & Bruce, 2007). Millipede development eventually locks the geometry. Intensification of the deformation at overall low strains is then only possible through the development of new millipedes that affect earlier formed ones at a smaller scale (e.g., Bell & Bruce, 2007). Smaller porphyroblasts can then grow without a change in the direction of bulk shortening. For clusters **I** and **III** in Fig. 2, we show a different phenomenon where three stages of andalusite growth during D_c (e.g., Figs 8d through 8h) occurred before the strain increased significantly and the overall deformation went significantly non-

coaxial and caused differentiated S_c to develop. This extended history resulted from the emplacement of coarse-grained replacive vein quartz across the first phase of D_c grown andalusite on the right side of the D_b core of **I** in Fig. 2 (Figs 2 & 3a). This increased competency parallel to the direction of bulk shortening, widened the zone of stronger material vertically. Strong localization of D_c was thus prevented against the top and bottom rims of D_c grown andalusite **I** and **III** in Fig. 8d and no differentiated S_c developed, allowing further D_c growth to occur as shown in Figs 8e & 8f. More growth followed immediately afterwards likely because of further vein emplacement in the third dimension and identifiable from the greater rotation of S_b towards S_c still without any differentiation (Figs 8g & 8h). Differentiation then followed causing further growth to cease (matrix of Fig. 8h). While this was going on ~4 cms away staurolite followed by andalusite were tracking components of an overall similar history but without the involvement of a quartz vein. Rather, the growth of 2 staurolite crystals about smaller scale newly developing millipedes made that location more competent and spread half millipede development laterally and below to result in andalusite growth.

V – 3. Timing from one porphyroblast encapsulating another

Prior to quantitative approaches using FIAs it was considered by a some researchers that a porphyroblast encapsulating another did not necessarily grow later but that has proven to be incorrect wherever quantitative FIA measurements have been made (Cihan & Parson, 2005; Sayab, 2005; Ali, 2009; Abu Sharib & Bell, 2011). In Fig. 4, although all porphyroblasts have the same FIA and all the core of **X** first grew during D_c , every staurolite in Fig. 4 predated the andalusite that encapsulates them. This is apparent from the fact that the millipede is differently and further developed in the surrounding andalusite than in staurolites **XI** and **XII** above the middle of the porphyroblast cluster. Furthermore, inclusion trails immediately below **XI** show curvature due to the vertical

shortening of matrix S_b against the lower surface of staurolite **XI** before andalusite overgrew them. Inclusion trails within the top of **X** match those in the adjacent andalusite above. They are the only portion of all trails within the 3 staurolite porphyroblasts that exclusively capture the clockwise non coaxial effects of D_c as it intensified. They suggest that the matrix above the core of **X** was shortening non-coaxially when that below was shortening coaxially. This is no surprise as millipede geometries are commonly better developed on one side of a porphyroblast than the other. The clockwise non-coaxial shortening is better shown by the bottom and top rim of the encapsulating andalusite that grew slightly later during D_c . It is worth pointing out that andalusite growth ceased as differentiated S_c developed in the matrix above and below (Bell et al., 1986).

V – 4.The implications of multiple phases of growth of both staurolite and andalusite

Classically, the multiple phases of growth of staurolite and andalusite revealed in Figs 2, 3, 4, 5, 8 & 9 are problematic. However, Thermocalc (Fig. 6) indicates they do coexist over a narrow PT range for the bulk composition of this sample and there is no evidence that either reacted to form the other in the 12 thin sections with different strikes cut from this sample. Intriguingly, they grew virtually simultaneously several times in the same thin section as well as in closely spaced portions of the same rock during the early stages of the three successive deformation events D_b , D_c and D_d . There is no problem with multiple phases of growth both within and from deformation to deformation if the past thirty years of detailed microstructural evidence is accepted. It shows that porphyroblast growth starts and stops totally as a function of how deformation partitions through rock as described and discussed above. Furthermore, this structural control has been thoroughly documented metamorphically by Sanislav & Bell

(2011) and Bell et al. (2013). Multiple growth of all porphyroblastic phases of minerals is common with examples routinely quantitatively documented using FIA data for garnet, staurolite, andalusite, cordierite and plagioclase.

V – 5. Inclusion trail variation in orientation due to porphyroblast rotation?

Johnson (2009) discarded the possibility that the two porphyroblasts he featured photographically had overgrown an already rotated foliation (Fig. 10) because he claimed there was no unequivocal evidence for it. Angular variance between inclusion trails in 2 or more porphyroblasts or 2 or more crystals within a cluster is typical of the effects of early coaxial bulk shortening (e.g., Figs 2, 4, 8 & 9). One needs to prove that such inclusion trail variation within single, adjacent or clusters of porphyroblasts did not occur prior to their growth since it is the expected product of the early bulk coaxial shortening that drives porphyroblast growth! T.H. Bell collected several immediately adjacent samples from a 1 metre square outcrop in the Robertson River Metamorphics because it contained the millipedes he featured in several papers. Johnson's (2009) photo is from one of those samples. The evidence for the development of millipede geometries and variation in millipede core trails prior to plagioclase growth due to bulk coaxial shortening, so significant in sample 43 described herein, is thoroughly documented for those samples in Bell & Bruce (2007).

REFERENCES

Adshead-Bell, N.S. & Bell, T.H., 1999. The progressive development of a macroscopic upright fold pair during five near orthogonal foliation production events: complex microstructures versus a simple macrostructure. *Tectonophysics*, **306**, 121-147

-
- Abu Sharib, A.S.A.A. & Bell, T.H., 2011. Radical changes in bulk shortening directions during orogenesis: significance for progressive development of regional folds and thrusts. *PreCambrian Research*, **188**, 1-20.
- Ali, A., 2010. The tectono-metamorphic evolution of the Balcooma Metamorphic Group, northeastern Australia; a multidisciplinary approach. *Journal of Metamorphic Geology*, **28**, 397-422.
- Bell, T.H. & Bruce, M.D., 2006. On the geometry of inclusion trails preserved within a first phase of porphyroblast growth. *Journal of Structural Geology*, **28**, 236-252.
- Bell, T.H. & Bruce, M.D., 2007. Progressive deformation partitioning and deformation history: Evidence from millipede structures. *Journal of Structural Geology*, **29**, 18-35.
- Bell, T.H. & Hayward, N., 1991. Episodic metamorphic reactions during orogenesis: the control of deformation partitioning on reaction sites and duration. *Journal of Metamorphic Geology*, **9**, 619-640.
- Bell, T.H. & Johnson, S.E., 1989. Porphyroblast inclusion trails: The key to orogenesis. *Journal of Metamorphic Geology*, **7**, 279-310.
- Bell, T.H. & Newman, R., 2006. Appalachian orogenesis: the role of repeated gravitational collapse. In: - Styles of continental compression, Eds R. Butler & S. Mazzoli, *Special Papers of the Geological Society of America* **414**, 95-118.
- Bell, T.H., Rieuwers, M.T., Cihan, M., Evans, T.P., Ham, A.P. & Welch, P.W., 2013. Inter-relationships between deformation partitioning, metamorphism and tectonism. *Tectonophysics*, **587**, 119-132.

- Bell, T.H. & Rubenach, M.J., 1983. Sequential porphyroblast growth and crenulation cleavage development during progressive deformation. *Tectonophysics*, **92**, 171-194.
- Bell, T.H. & Sapkota, J., 2012. Episodic gravitational collapse and migration of the mountain chain during orogenic roll-on in the Himalayas. *Journal of Metamorphic Geology*, **30**, 651-666.
- Bell, T.H. & Sanislav, I.V., 2011. A deformation partitioning approach to resolving the sequence of fold events and the orientations in which they formed across multiply deformed large-scale regions. *Journal of Structural Geology*, **31**, 1206-1217.
- Biot, M.A. 1957. Folding instability of a layered viscoelastic medium under compression. *Proceedings of the Royal Society of London*, **A242**, 111-454.
- Biot, M.A. 1965. *Mechanics of Incremental Deformations*. John Wiley, New York. 504pp.
- Bruce, M.D., 2007. Unpublished PhD Thesis, James Cook University.
- Cihan, M. & Parson, A. 2005. The use of porphyroblasts to resolve the history of macro-scale structures: an example from the Robertson River Metamorphics, North-Eastern Australia. *Journal of Structural Geology*, **27**, 1027–1045.
- Fleming, P.D., 1971. Metamorphism of Folding in the Mt Lofty Ranges, South Australia, with Particular Reference to the Dawesley–Kanmantoo Area. *Unpubl. Ph.D. Thesis, University of Adelaide*, 316 pp.
- Foden, J.D., Turner, S.P. & Morrison, R.S., 1990. Tectonic implications of Delamerian magmatism in South Australia and western Victoria. In: J.B. Jago and P.S. Moore (Editors), *The Evolution of a Late Precambrian-Early Palaeozoic Rift Complex: The Adelaide Geosyncline*. *Geol. Soc. Aust., Spec. Publ.*, **16**, 465-482.

-
- Ham, A.P. & Bell, T.H., 2004. Recycling of foliations during folding. *Journal of Structural Geology*, **26**, 1989-2009.
- Johnson, S.E., 2009. Porphyroblast rotation and strain localization: Debate settled! *Geology*, **37**, 663-666.
- Offler, R., 1966. The Structure and Metamorphism of the PewseyVale Area, Northeast of Williamstown, South Australia. *Unpubl.Ph.D. Thesis, University of Adelaide*, 128 pp.
- Offler, R. & Fleming, P.D., 1968. A synthesis of folding and metamorphism in the Mt. Lofty Ranges, South Australia. *J.Geol. Soc. Aust.* **15**, 245–266.
- Mills, K., 1964. The Structural Geology of an Area East ofSprington, South Australia. *Unpubl. Ph.D. Thesis, University of Adelaide*, 497 pp.
- Ramberg, H. 1963. Fluid dynamics of viscous folding. *Bulletin of the American Association of Petroleum Geologists*, **47**, 484-515.
- Rich, B.H., 2005. Unpublished PhD Thesis, James Cook University.
- Sanislav, I.V. & Bell, T.H., 2011. The inter-relationships between long-lived metamorphism, pluton emplacement and changes in the direction of bulk shortening during orogenesis. *Journal of Metamorphic Geology*, **29**, 513-536.
- Sayab, M., 2005. N-S shortening during orogenesis within the Mt Isa Inlier (NW Queensland, Australia): the preservation of early W-E trending foliations in porphyroblasts revealed by independent 3D measurement techniques. *Journal of Structural Geology*, **27**, 1445-1468.
- Weinberg R. & Hasalova, P., 2014. Multiple Melting Events During an Orogeny and the Role of Water. *Geophysical Research Abstracts*, **16**, EGU 2014-2981.
- Yeh, M._W., 2001. Unpublished PhD Thesis, James Cook University.

- CHAPTER IV -

THE SIGNIFICANCE FOR METAMORPHISM, OROGENESIS AND

PT PATHS OF ~40 MILLION YEARS OF MULTIPLE PHASES OF

DEFORMATION AND EFFECTIVELY SYNCHRONOUS

STAUROLITE-ANDALUSITE GROWTH

- CHAPTER IV -

THE SIGNIFICANCE FOR METAMORPHISM, OROGENESIS AND PT PATHS OF ~40

MILLION YEARS OF MULTIPLE PHASES OF DEFORMATION AND EFFECTIVELY

SYNCHRONOUS STAUROLITE-ANDALUSITE GROWTH

ABSTRACT.....	93
I - INTRODUCTION.....	94
II - STRUCTURAL AND METAMORPHIC BACKGROUND.....	95
III - DATA.....	96
III - 1.Sample locations and distribution of mineral assemblages.....	96
III - 2.Deformation history recorded by the FIAs.....	96
III - 3.Staurolite-Andalusite samples with the same FIAs.....	97
III - 4.P-T Pseudosections.....	98
IV - INTERPRETATION.....	99
IV - 1.Microstructural evidence of multiple growth events of co-stable staurolite/andalusite	99
IV - 2.T-P space for coexisting staurolite and andalusite.....	99
IV - 3.Garnet distribution and PT paths.....	100
V- DISCUSSION.....	102
V - 1.Lengthy coexistence of staurolite and andalusite	102
V - 2.Reasons for multiple staurolite-andalusite growth	103
V - 2.1 Switching porphyroblast growth on and off.....	103
V - 2.2 P-T loops and reoccurrence of metamorphic reactions	103
V - 2.3 Role of external fluids	104

V - 3. Geodynamic implications of a similar stability field in PT space over time..	104
V - 3.1 Multiple orogenesis yet confined PT space	104
V - 3.2 Relative stability versus fast exhumation rates.....	105
REFERENCES	107

ABSTRACT

The southern portion of the Adelaide fold belt contains a large region where synchronous to interleaved growth of staurolite and andalusite porphyroblasts has occurred. The truncation and continuity of inclusion trails versus matrix foliations reveal multiple periods of growth of staurolite and andalusite in many samples. The measurement of FIAs (foliation intersection axes preserved within porphyroblasts) revealed a succession of 5 changes in the bulk shortening direction during orogenesis from initially NNW-SSE when the first FIA (I), trending at 75°, formed in garnet. FIAs II through V are present in garnet, staurolite and andalusite. Indeed, staurolite and andalusite grew in the same sample during the development of at least one of FIAs II, III, IV and V. Pseudosections show a remarkably narrow range of PT conditions where this is possible and define a very confined location in PT space where these rocks developed at least 10 foliations over the ~ 30 million years that FIAs II through V developed. Garnet growth occurred early in some samples, but not in others with very similar bulk chemistry, where staurolite and andalusite grew in the same FIA event. This behaviour resulted from slight changes in Mn content and allowed a very tightly constrained PT path to be defined on pseudosections in combination with the minerals that formed early and late in some multi FIA samples. These low-pressure high-temperature rocks remained at the same orogenic level throughout most of the very lengthy deformation history of the Delamerian orogenic cycle once staurolite and andalusite began to grow. They ceased to grow at the commencement of exhumation when retrogressive chlorite growth began in many samples when shortening was directed once again NNW-SSE.

Keywords: staurolite and andalusite co-stability; FIAs; multiple phases of metamorphism; PT stability during orogenesis

I - INTRODUCTION

The bulk of the Adelaide geosyncline appears relatively simple structurally at both macroscopic and mesoscopic scales due to large, upright, open, double plunging folds and an upright axial plane slaty cleavage (Bell, 1978). Locally, in high metamorphic grade parts of the orogen, three deformation events have been described (Offler, 1963, 1966; Offler & Fleming, 1968). Foliations preserved as inclusion trails in cordierite and andalusite porphyroblasts (Steinhardt, 1989) and these phases plus garnet and staurolite reveal a minimum of five deformation events in the southern Mount Lofty Range (Adshead-Bell & Bell, 1999). Successive bulk shortening axes associated with these foliations appear near orthogonal in cross-section with periods of staurolite and andalusite growth occurring early during at least four of the deformation events (Adshead-Bell & Bell, 1999).

Such multiple growths of the latter two porphyroblastic phases potentially leads to conflict between metamorphic and structural geologists. Most metamorphic petrologists argue that when the required PT is reached or overstepped for a particular bulk composition, any associated metamorphic reaction causing porphyroblast growth goes to completion in one event (Spear, 1993). Yet foliations preserved as inclusion trails in both these porphyroblasts display a range of morphologies, overprinting relationships and orientations that microstructurally indicate multiple growth of both of these phases (e.g., Bell & Hickey, 1999; Ali, 2010; Sanislav & Shah, 2010; Quentin de Gromard, 2013). One approach to resolving this contradiction is that the re-occurrence of porphyroblast growth other than garnet involved the remobilisation of solutes from external source, e.g., metasomatic fluids (Rubenach & Baker, 1998; Rubenach, 2005). Alternatively, it has long been argued that crystal growth ceases once differentiation

during crenulation cleavage development occurs against a given porphyroblast (Spiess & Bell, 1996; Sanislav & Bell, 2011). They suggest this prevents components needed for the metamorphic reaction from being exhausted in a single growth event, allowing them to be reused in a later event and is supported by significant foliation age progressions from porphyroblast cores to rims and FIAs (Bell & Welch, 2002; Ali, 2010; Sanislav, 2011; Abu Sharib & Sanislav, 2013). It explains episodic growth of porphyroblasts with no change in the metamorphic reaction that produces them. Significantly, FIAs (Foliation Intersection/Inflexion Axes preserved in porphyroblasts) defined by such foliation progressions define lengthier deformation and metamorphic histories missed if matrix and inclusion trail foliation successions alone are taken into consideration (Aerden & Sayab, 2008; Quentin de Gromard, 2013).

II - STRUCTURAL AND METAMORPHIC BACKGROUND

The lengthy tectono-metamorphic history of the Kanmantoo group is attested by the abundance of granites with ages ranging from 525 Ma to 475 Ma that outline the structural trends of the Adelaide Geosyncline (Fig. 1a). Those following the North-South arm of this orogen in Fig. 1a have ages ranging from 510Ma to 475Ma (Fig. 1b) and those following the West-East trend of the western arm range from 525 Ma to 500 Ma (Fig. 1c).

The sedimentary nature of the protolith varies from mudstones through siltstone and sandstones to greywackes (Fig. 2). Metamorphism in the Kanmantoo group is classically portrayed as Buchan type characterized by low to medium pressure and medium to high temperature assemblages such as staurolite, andalusite, sillimanite (fibrolitic and prismatic) and potassic feldspar. Metamorphic grade is commonly described as increasing from West to East with a shift from andalusite + staurolite to

fibrolitic sillimanite, then prismatic sillimanite and finally migmatite (Mills, 1964; Offler and Fleming, 1968; Dymocke and Sandiford, 1992; Oliver et al., 1998).

III - DATA

III - 1. Sample locations and distribution of mineral assemblages

The mineral assemblage zones shown in Fig. 3 were established by analysing multiple thin sections cut from each of the 109 samples collected across the southern Mount Lofty Range (Fig. 2). The matrix foliation is generally defined by quartz, biotite and muscovite. Garnet is irregularly distributed (Fig. 3a), there is a large area of rocks with stable staurolite and andalusite (Fig. 3b), and fibrolitic sillimanite is common throughout this zone (Figs. 3c & 3d), having locally formed within biotite (Fig. 4). Coarse tabular muscovite grains crosscut the foliation (Fig. 5a, b) and locally replace staurolite and andalusite (Fig. 6c). Late chlorite locally replaces biotite along (001) (Fig. 4a) and can be coarser grained as rosettes or late porphyroblasts in very late open crenulation hinges (Fig. 6b) that preserve a different FIA trend.

III - 2. Deformation history recorded by the FIAs

Chapter 2 contains a detailed description of the FIA method and the results obtained by measuring FIAs in garnet, staurolite and andalusite porphyroblasts. When plotted on a rose diagram, five peaks trending WNW-ESE, NNW-SSE, SSW-NNE, SW-NE and WSW-ENE were identified as shown in Fig. 7. The data includes 20 FIAs measured from staurolite porphyroblasts, 21 FIAs measured from andalusite porphyroblasts and 7 FIAs measured from garnet porphyroblasts. Changes in FIA trend from the core to the rim of porphyroblasts were used to establish the relative timing between different FIA sets. The resulting succession (Chapter 2) indicates that WSW-ENE trending FIAs were followed by those trending NNW-SSE, WNW-ESE, SSW-NNE and finally SW-NE (Fig. 7) with the last 4 occurring in all 3 phases and the first only in garnet. These

changes in trend reflect shifts in plan view of the large-scale bulk shortening direction (which lies orthogonal to the FIA, Bell & Newman, 2006) with time. The distribution and succession of FIAs I through V (Fig. 7) can be linked to the distribution of fold axial planes throughout the Adelaide geosyncline allowing reconstruction the succession of deformation events responsible for the overall S-shape of the orogen (e.g., Chapter 2).

III - 3. Staurolite-Andalusite samples with the same FIAs

Samples 10, 16, 19, 43, k22 and k23 all contain an identical FIA in both staurolite and andalusite (highlighted in orange in Fig. 8) and samples 10 and 19 contain different FIAs in at least one of those phases (Fig. 8). For example, the inclusion trails in staurolite cores in sample 19 define FIA IV whereas FIA V is present in staurolite rims and both the cores and rims of andalusite porphyroblasts. Thus for this sample the porphyroblast sequence consists of a first growth of staurolite during FIA IV followed by coeval growth of staurolite and andalusite during FIA V.

At least 3 foliations defining the same FIA (FIA II) in sample 16. Looking North the foliation asymmetries define a staircase asymmetry (Bell & Johnson, 1992) with the first formed steep to flat asymmetry preserved in andalusite and the second flat to steep asymmetry seen in both andalusite and staurolite. Therefore, the mineral succession for this sample consists of a phase of andalusite growth followed by coeval growth of both andalusite and staurolite.

The inclusion trails in both staurolite and andalusite in Sample 43 also resulted from 3 distinct phases of growth during 3 deformation events around the same FIA trend, but define a spiral asymmetry. This has implications for the inter-relationships between deformation and metamorphism other than those described in this paper that are described and interpreted in detail in Chapter 3.

Table 8 shows that FIAs II, III, IV and V are present in both staurolite and andalusite in samples 16, 10, 43/k22/k23 and 19 respectively. Since at least 2 phases of growth of andalusite or staurolite over different foliations are present in samples 10, 19, k22 and k23, and 3 are present in 16 and 43, there have been at least 10 phases of foliation development during the development of the last 4 FIAs.

III - 4.P-T Pseudosections

Pseudosections were modelled for the 6 samples with the same FIAs in co-existing staurolite and andalusite mentioned above. They were also conducted for one containing sillimanite but no staurolite or andalusite (sample 28). The pseudosections were constructed in the MnNCKFMASH system using Powell's & Holland's (1988) Thermocalc software. The bulk compositions for major elements of these 8 samples (Fig. 9) were determined by quantitative XRF analysis at the JCU Advanced Analytical Centre (for samples 43, k22, k23) and AMDEL Bureau veritas (for samples 10, 16, 19, 28). The phase calculations were obtained using the Holland & Powell (1998) dataset (tvd55.txt, November 2003 update), Tinkham et al. (2001) mixing models, the Coggon & Holland (2002) activity model for muscovite, and the Holland & Powell (2003) ones for feldspar. The following phases were taken into account: quartz, chlorite, zoisite, muscovite, plagioclase, k-feldspar, biotite, garnet, staurolite, andalusite, sillimanite, kyanite, cordierite and H₂O. Samples were modelled in a 1 to 9 Kbar and 400 to 750°C range, with quartz, plagioclase and water set as excess phases. The pseudosections for all 7 samples are shown in Fig. 10a & b.

IV - INTERPRETATION**IV - 1. Microstructural evidence of multiple growth events of co-stable staurolite/andalusite**

At least four different FIA trends were measured in samples that contain texturally stable staurolite and andalusite. Thus at least 4 phases of co-stable andalusite and staurolite growth coeval with 4 different FIA events are preserved in 6 of the seven samples described herein. Indeed, 3 phases of both staurolite and andalusite growth occurred within sample 16 during FIA II and sample 43 during FIA IV; the techniques for determining this from the microstructures are described in detail for sample 43 in Chapter 3. Combining these with growth in FIA sets III and V (Fig. 8) indicates a minimum of 6 co-stable to interleaved phases of growth of staurolite and andalusite porphyroblasts. This number likely to be higher as 8 across the region because multiple stages of growth of staurolite and andalusite in FIA stages III and V have also occurred (e.g., the staurolite in Fig. 6a,b contains FIAs IV and V).

IV - 2. T-P space for coexisting staurolite and andalusite

The pseudosections for samples 10, 16, 19, 43, k22 and k23 in Fig. 10a & b, which contain at least one FIA the same in coexisting staurolite and andalusite, show a field in PT space that include both these phases. Figures 11a, b, c, d, e and f magnify this field with Fig. 11g combining all 6 onto the one plot. The total variation in P-T space where they coexist is small, ranging over a maximum of 1kb and 30°C (Fig. 11g) centred on 3.77kb and 565°C. Indeed, the range is not that much smaller if the outlier sample, 10, is excluded at 0.65kb and 26°C centred on 3.88kb and 567°C (Fig. 12b). Samples 10, 16 and 19 lie within 2.5 kms of one another (Fig. 2) and contain FIAs III, II and V respectively in staurolite and andalusite (Fig. 8). Samples 10 and 19 contain FIA II in andalusite and IV in staurolite respectively. The development of each FIA involves a

minimum of 2 periods of foliation development, and most commonly at least 3 (Bell & Sapkota, 2012; Bell et al., 2013). For example, 4 are preserved in sample 43 with staurolite and andalusite growing during the last 3 of those (Chapter 3). Consequently, this narrow PT range likely occurred during the development of a minimum of 10 deformation events over this 2.5 km distance. The residence time of these rocks at that depth during orogenesis was therefore significant and at least 30 million years based on the distribution of granites versus FIAs versus orocline shape described in Chapter 2.

IV - 3. Garnet distribution and PT paths

Offler and Fleming (1968) observed that garnet porphyroblasts have an unusual geographic distribution in this area (Fig. 3a). Garnet is generally one of the first porphyroblastic phases that grow in metamorphic terranes. Furthermore, being refractory, early garnet growth is commonly preserved during later prograde metamorphic events in staurolite and andalusite bearing meta-pelites. In the South Mount Lofty Ranges, garnet bearing rocks are located in patches that do not define an obvious isograd (Fig. 3a). The AFM projection in Fig. 13 suggests the bulk chemical compositions of samples 19, 28, 43, k22 and k23 are somewhat similar yet only 19 contains garnet. However, their pseudosections differ significantly in some cases (Fig. 10). Figure 13 suggests that the chemical composition of samples 19, 28, 43, k22 and k23 are the most similar and their pseudosections show similarities. Samples 19, 43, k22 and k23 are very similar mineralogically containing staurolite, andalusite and minor fibrolite except that 19 also contains garnet. Figure 13 suggests the garnet distribution within these four did not result from significant differences in the rock bulk chemistry. Rather, the answer appears to lie in the low manganese contents of k22, k23 and 43 vs the much higher amount in 19 (Figs 14a & 14b; see below). The mineral assemblage in sample 28 (includes microcline, fibrolite and late muscovite plus the porphyroblastic

phases in Fig. 8) indicates that this rock reached significantly higher temperatures and possibly pressures (655-710 °C, 3.8-5.7 kb Fig. 10b). An anticlockwise PT path (e.g., Alias et al., 2002; see below) through the pseudosection in Fig. 10b would readily account for the lack of garnet.

Calculation using Thermocalc of the mineral stability field around the PT area where the garnet, staurolite and andalusite in-lines intersect provides an answer as to why garnet does not occur in samples k22 and k23. It also points to a solution as to why there is no garnet in sample 43 and yet the pseudosection (Figs 10a, 11d & 15c) indicates that there should be. The pseudosections for k22 (Figs 10b, 11e & 15a,) and k23 (Figs 10b, 11f & 15b) show that the garnet in-lines deviate away from the staurolite-andalusite co-stable zone. This results in a small PT path window where staurolite and andalusite are co-stable but garnet is not (Fig. 15a,b) and would not grow along the PT path shown. Along any other path it would have grown. The pseudosection for sample 43 (Fig. 15c) suggests staurolite and andalusite should coexist with garnet. This sample contains many large andalusite and small to medium sized staurolite porphyroblasts that grew overall synchronously during the development of 3 deformation events (Chapter 3). However, no garnet was found in the 12 differently oriented thin sections cut from this rock or is visible in the rock itself. The lack of garnet appears to lie in the molar proportion of MnO in this sample shown in Fig. 14a. At 0.09 it lies between samples 10 and K23 whose pseudosections respectively suggest garnet does and does not accompany staurolite plus andalusite. Calibration of the sensitivity to Mn content within Thermocalc may need slight adjustment.

The near synchronous and multiple growth phases of staurolite and andalusite in sample 43 (Chapter 3) indicate a PT path not dissimilar to that for k22 and k23 as shown in Fig. 15a,b,c. This is supported by the higher Mn content (Fig. 14a) and the

resultant pseudosection for sample 19 (Fig. 11c) where garnet grew early, followed by andalusite (FIA II) staurolite (FIA III), then by further growth of both these phases during FIA IV. The latest transition from cordierite to sillimanite for sample 19 is consistent with this clear ACW TP path with time. Figure 16 shows this information combined onto a single plot. The combination of the information from k22, k23, 43 and 19 reveals a well-constrained ACW PT path in accordance with the one inferred to the South in Petrel Cove by Alias et al (2002). The path for 28 is somewhat similar but started at much higher temperature due to its proximity to granite.

V- DISCUSSION

V - 1.Lengthy coexistence of staurolite and andalusite

Staurolite and andalusite occur together in many samples from the Kanmantoo region. Figure 11g shows that they stably coexist only over a limited PT range that is similar from sample to sample. Yet these samples are spread more than 20 kms across the Kanmantoo region and grew over a lengthy deformation history involving the development of at least 10 foliations. Consequently, any variations in temperature and pressure resulting from switching from bulk horizontal shortening to gravitational collapse were less than 1 kb and 30°C for all six samples in Fig. 11; they were even more tightly constrained for the 5 samples whose range overlapped (Fig. 11g). This pseudosection observation is supported by the lack of evidence for any reaction between juxtaposed staurolite and andalusite. It is strengthened by a total lack of phases amongst the inclusions defining the foliations preserved within andalusite and staurolite cores versus medians versus rims that could have grown and thus been included if reactions due to variation in PT had taken place during the deformations controlling these stages of growth (Chapter 3).

V - 2.Reasons for multiple staurolite-andalusite growth

The three potential solutions are that 1) the reaction takes many deformation events to reach completion, 2) the rock oscillates around the staurolite-andalusite co-stability field or 3) solutes are pumping through the rock due to metasomatism.

V - 2.1 Switching porphyroblast growth on and off

Bell & Hayward (1991) and Spiess & Bell (1996) argued that the growth of a porphyroblast phase stops once differentiated cleavage begins on its margin because access of the components needed for growth, as well as the removal of those that are superfluous, ceases. Microfracture within phyllosilicates and along their boundaries with other minerals readily explains the early timing of porphyroblast growth during the initial coaxial stages of bulk shortening (Bell & Hayward, 1991) and the sub-vertical sub-horizontal dominance of most inclusion trails (Bell & Newman, 2006), especially those forming against an earlier formed core (Bell & Sapkota, 2012). Geometric strain softening once differentiation begins and cessation of microfracture explains why growth ceases (Bell & Bruce, 2007). Consequently the reaction does not go to completion and can recommence in a later deformation event. This has been quantitatively demonstrated by Sanislav & Bell (2011) and is strongly supported by monazite dating of a FIA succession (Sanislav, 2011) where four staurolite growth events occurred from 410 Ma to 345 Ma in the northern Appalachians. It is further quantitatively supported by the extraordinary differences in the timing of initial growth of garnet through the same succession of FIA events between the Chester and Pomfret domes in Vermont (Bell et al., 2013).

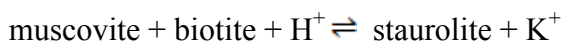
V - 2.2 P-T loops and reoccurrence of metamorphic reactions

Slight variations of temperature and pressure may cause the rock to oscillate around the P-T zone fertile for the growth of staurolite and andalusite. For instance, in the pseudo-

section of sample 43 (Figs 10a, 11d and 15c), an increase in PT would cause andalusite to react out leaving staurolite behind. An increase of P alone at lower temperatures could break andalusite down and form chlorite and an increase in T alone could react out staurolite. With a backwards flux of any of these increases andalusite or staurolite could regrow. However, no criteria were found that indicate such a cycling. Furthermore, the pseudosections define a distinct field where both andalusite and staurolite could grow and exist together in equilibrium. Of course, there is evidence of breakdown of andalusite and staurolite to muscovite and chlorite once retrogression began but that is always post the growth of both the former phases. In particular chlorite was never included as trails overgrown by andalusite or staurolite in any of the rocks examined across this region during any phase of growth in any FIA event.

V - 2.3 Role of external fluids

Fluids pumping through this rock over time have been suggested as a possible cause via reactions such as



(Rubenach & Baker, 1998; Arnold et al., 2000).

Yet little albite growth or other evidence for a significant role for metasomatism occurs in the rocks from this area that preserve multiple growths of andalusite and staurolite.

V - 3. Geodynamic implications of a similar stability field in PT space over time

V - 3.1 Multiple orogenesis yet confined PT space

The succession of 5 changes in FIA trend in this region indicate at least 5 changes in the direction of bulk horizontal shortening during ~40 million years of orogenesis (Chapter 2) due to shifts in the direction of relative plate motion (e.g., Bell & Sapkota, 2012). FIAs II, III, IV and V which resulted from the development of at least 8 and more likely 10 foliations, are preserved in rocks containing stable assemblages of staurolite and

andalusite that are tightly clustered in PT space (Figs 11 & 12). Such a rich tectono-metamorphic history could appear to be in contradiction with the crustal stability of these rocks over most of the delamerian orogeny. Many authors relate a shortening event responsible for a development of a metamorphic fabric to significative vertical transport and flux of the rocks within the crust (Stipska et al., 2008; Skrzypek et al., 2011; Stipska et al., 2012). To the contrary this study shows that although multiply deformed the overall displacement of these rocks is minimum. All porphyroblasts preserve successions of predominantly steeply and gently pitching foliations in thin sections at most angles to the FIA trend suggesting they are sub-vertical and sub-horizontally dipping (c.f., Bell & Newman, 2006; Bell & Sapkota, 2012). Consequently, the crust moved up or down only a few hundred metres from deformations producing sub-vertical foliations to those producing sub-horizontal foliations over at least 8 periods of deformation and many millions of years for FIAs II to V. More periods of multiple deformation occurred during the development of FIAs I (only in garnet). This suggests a near balance being achieved by early FIA II between topographic height, isostasy and erosion above the orogen core that resulted from collisional relative plate motion vs phases of gravitational collapse within the top 18 to 30 kms of highest standing crust (e.g., Bell & Sapkota, 2012).

V - 3.2 Relative stability versus fast exhumation rates

Rapid exhumation rates are common for rocks now at the surface in modern orogens such as the Himalayas (Guillot et al., 2008; Guillot et al., 2009). Monazite inclusions in garnet porphyroblasts at the surface near the MCT and in the Central Nepal Himalayas, date between 45 and 19 Ma. Yet, from 45 to ~19 Ma, these garnets did not shift significantly in PT space during the development of a succession of 15 sub-vertical and sub-horizontal foliations. This resulted from the fact that exhumation rates speed up

almost exponentially as rocks begin to move significantly away from deep in the orogen core due the geometric effects of vertical bulk shortening during gravitational collapse (see fig. 8 in Bell & Sapkota, 2012).

REFERENCES

- Abu Sharib, A.S.A.A, Sanislav, I.V, 2013. Polymetamorphism accompanied switching in horizontal shortening during Isan Orogeny: Example from the Eastern Fold Belt, Mount Isa Inlier, Australia. *Tectonophysics*, **587**, 146-167.
- Adshead-Bell, N.S., Bell, T.H. 1999. The progressive development of a macroscopic upright fold pair during five near-orthogonal foliation-producing events: complex microstructures versus a simple macrostructure. *Tectonophysics*, **306**, 121-147.
- Aerden, D., Sayab, M., 2008. From Adria – to Africa-driven orogenesis: evidence from porphyroblast in the Betic Cordillera, Spain. *Journal of Structural Geology* , **30**, 1272-1278.
- Ali, A., 2010. The tectono-metamorphic evolution of the Balcooma Metamorphic Group, north-eastern Australia: a multidisciplinary approach. *Journal of Metamorphic Geology*, **28**, 397-422.
- Alias, G, Sandiford, M., Hand, M, Worley, B, 2002. The T-P record of synchronous magmatism, metamorphism and deformation at Petrel Cove, southern Adelaide Fold Belt. *Journal of metamorphic geology*, **20**, 351-363.
- Arnold, J., Powell, R., Sandiford, M., 2000, Amphibolites with staurolites and other aluminous minerals: calculated mineral equilibria in NKFMAASH. *Journal of metamorphic Geology*, **27**, 679-678.
- Bell, T.H., 1978. The development of slaty cleavage across the Nackara Arc of the Adelaide Geosyncline. *Tectonophysics*, 51,171–201.
- Bell, T.H., Hayward, N., 1991. Episodic metamorphic reactions during orogenesis: the control of deformation partitioning on reaction sites and duration. *Journal of metamorphic geology*, **9**, 619–640.

-
- Bell, T. H., & Johnson, S. E. (1992). Shear sense. *Journal of Metamorphic Geology*, **10(1)**, 99-124.
- Bell, T.H. & Hickey, K.A., 1999. Complex microstructures preserved in rocks with a simple matrix: significance for deformation and metamorphic processes. *Journal of Metamorphic Geology*, **17**, 521-536.
- Bell, T.H., Welch, P.W., 2002. Prolonged Acadian orogenesis: revelation from foliation intersection axis (FIA) controlled Monazite dating of foliations in porphyroblasts and matrix. *American journal of science*, **302**, 549-581.
- Bell, T.H., Newman, R., 2006. Appalachian orogenesis: the role of repeated gravitational collapse. In: Butler, R, Mazzoli, S(eds), Style of Continental Compression. *Geological society of America Special Papers*, **414**, 95-118.
- Bell, T.H., Bruce, M.D., 2007. Progressive deformation partitioning and deformation history: evidence from millipede structures. *Journal of Structural Geology*, **29**, 18-35.
- Bell, T.H., Sapkota, J., 2012. Episodic gravitational collapse and migration of the mountain chain during orogenic roll-on in the Himalayas. *Journal of metamorphic geology*, **30**, 651-666.
- Bell, T.H., Rieuwers, M.T., Cihan, M., Evans, T.P, Ham, A.P., Welch, P.W., 2013. Inter-relationship between deformation partitioning, metamorphism and tectonism. *Tectonophysics*, **587**, 119-132.
- Coggon, R., Holland, T.J.B., 2002. Mixing properties of phengitic micas and revised garnet-phengite thermo-barometers. *Journal of Metamorphic Geology*, **7**, 503-506.

- Dymocke, P., Sandiford, M., 1992. Phase reactions of Buchan facies series pelitic assemblages: calculations and application to the Mount Lofty Ranges, South Australia. *Contrib. Mineral Petrol*, **110**, 121-132.
- Guillot, S., Mahéo, G., De Sigoyer, J., Hattori, K. H., Pecher, A., 2008. Tethyan and Indian subduction viewed from the Himalayan high-to ultrahigh-pressure metamorphic rocks. *Tectonophysics*, **451**, 225-241.
- Guillot, S., Hattori, K., Agard, P., Schwartz, P., Vidal, O., 2009. Exhumation processes in oceanic and continental subduction contexts: a review. In *Subduction zone geodynamics*, pp. 175-205. Springer Berlin Heidelberg.
- Holland, T.J.B., Powell, R., 1998. An internally consistent thermodynamic data set for phases of petrological interest. *Journal of Metamorphic Geology*, **16**, 309-343.
- Holland, T.J.B., Powell, R., 2003. Activity-composition relations for phases in petrological calculations: an asymmetric multicomponent formulation. *Contribution to Mineralogy and Petrology*, **145**, 1237-1259.
- Mills, K., 1964. The Structural Geology of an Area East of Springton, South Australia. Unpubl. Ph.D. Thesis, University of Adelaide, 497 pp.
- Munro, M. A., Blenkinsop, T. G., 2012. MARD—A moving average rose diagram application for the geosciences. *Computers & Geosciences*, **49**, 112-120.
- Offler, R., 1963. Structural geology of the Strathalbyn Anticline, South Australia. *Trans. R. Soc. S. Aust.*, **87**, 199–208.
- Offler, R., 1966. The Structure and Metamorphism of the Pewsey Vale Area, Northeast of Williamstown, South Australia. Unpubl. Ph.D. Thesis, University of Adelaide, 128 pp.
- Offler, R., Fleming, P.D., 1968. A synthesis of folding and metamorphism in the Mt. Lofty Ranges, South Australia. *J. Geol. Soc. Aust.*, **15**, 245–266.

- Oliver, N.H.S., Dipple, G.M., Cartwright, I., Schiller, J., 1998. Fluid flow and metasomatism in the genesis of the amphibolite-facies, pelite-hosted Knamantoo copper deposit, South Australia. *Am. J. Sci.*, **298**, 181-218.
- Powell, R., Holland, T.J.B., 1988. An internal consistent dataset with uncertainties and correlations; 3, Applications to geobarometry, worked examples and a computer program. *Journal of Metamorphic Geology*, **6**, 173-204.
- Quentin de Gromard, R., (2013). The significance of E–W structural trends for the Alice Springs Orogeny in the Charters Towers Province, North Queensland. *Tectonophysics*, **587**, 168-187.
- Rubenach, M.J., Barker, A.J., 1998. Metamorphic and metasomatic evolution of the Snake Creek Anticline, Mount Isa Inlier. *Australian Journal of Earth Science*, **45**, 363 -372.
- Rubenach, M.J., 2005. Relative timing of albitization and chlorine enrichment in biotite in Proterozoic shists, snake creek anticline, Mount Isa inlier, Northeastern Australia. *The Canadian mineralogist*, **43**, 349-366.
- Sanislav, I.V. & Shah, A.A., 2010. The problem, significance and implications for metamorphism of 60 million years of multiple phases of staurolite growth. *Journal of the Geological Society of India*, **76**, 384-398.
- Sanislav, I.V., 2011. A long-lived metamorphic history in the contact aureole of Mooselookmeguntic pluton revealed by in situ dating of monazite grains preserved as inclusions in staurolite porphyroblasts. *Journal of Metamorphic Geology*, **29**, 251-273.
- Sanislav, I.V., Bell, T.H., 2011. The inter-relationships between long-lived metamorphism, pluton emplacement and changes in the direction of bulk shortening during orogenesis. *Journal of metamorphic geology*, **29**, 513-536.

- Spear, F.A., 1993. Metamorphic phase equilibria and Pressure-Temperature-time paths. *Mineralogical society of America*, Monograph series, 799p.
- Spiess, R., Bell, T.H., 1996. Microstructural controls on the rate of metamorphic reaction: a case study of the inter-relationship between deformation and metamorphism. *European Journal of Mineralogy*, **8**, 165-186.
- Skrzypek, E., Štípská, P., Schulmann, K., Lexa, O., & Lexova, M., 2011. Prograde and retrograde metamorphic fabrics—a key for understanding burial and exhumation in orogens (Bohemian Massif). *Journal of Metamorphic Geology*, **29**, 451-472.
- Štípská, P., Schulmann, K., & Powell, R., 2008. Contrasting metamorphic histories of lenses of high-pressure rocks and host migmatites with a flat orogenic fabric (Bohemian Massif, Czech Republic): a result of tectonic mixing within horizontal crustal flow?. *Journal of Metamorphic Geology*, **26**, 623-646.
- Štípská, P., Chopin, F., Skrzypek, E., Schulmann, K., Pitra, P., Lexa, O., & Žáčková, E., 2012. The juxtaposition of eclogite and mid-crustal rocks in the Orlica–Śnieżnik Dome, Bohemian Massif. *Journal of Metamorphic Geology*, **30**, 213-234.
- Steinhardt, C.K., 1989. Lack of porphyroblast rotation in noncoaxially deformed schists from Petrel Cove, South Australia, and its implications. *Tectonophysics*, **158**, 127-140.
- Tinkam, D.K., Zuluaga, C.A., Stowell, H.H., 2001. Metapelite phase equilibria modelling in MnNCKFMASH: the effect of variable Al₂O₃ and MgO/(MgO + FeO) on mineral stability. *Geological Material Research*, **3**, 1-35.

GENERAL CONCLUSIONS

This study tested the continuum mechanics validity of the non-rotation model for porphyroblast growth and behaviour associated with transitions from coaxial to non-coaxial strain as the deformation intensified. It tested the ability of FIAs to resolve the structural history of an oroclinal orogen. It reveals that a detailed study of inclusion trail geometry provides much data on the timing of successive periods of porphyroblast growth as well as different mineral phases relative to coaxial versus noncoaxial behaviour as the deformation intensifies to form differentiated crenulation cleavages. Significant amongst these data was recognition of a significant role for millipeding in the development of a spiral-shaped inclusion trail geometry. It revealed that FIAs in combination with pseudosections provides a powerful approach for the determination of tightly constrained PT paths that developed during at least ten ductile deformation events over more than 40 million years. Furthermore, during this time, 5 dramatic changes in the direction of bulk shortening and thus the direction of relative plate motion occurred.

The principal findings of each chapter are synthetised below:

Chapter I

The numerical experiments described in chapter I show that if a significant amount of pure shear (35% of shortening) is applied to a model containing competent objects prior to subsequent simple shear or inhomogeneous bulk shortening, the object does not rotate if it is not internally deformed. Indeed, this approach was the first to provide a solution in continuum mechanics for a lack of porphyroblast rotation during non-coaxial strain. Near coaxial bulk shortening produces a millipede geometry, which if partially overgrown by a porphyroblast prevents subsequent rotation as the deformation intensifies and becomes non-coaxial. That is, the strain localizes within the

millipede geometry, leaving the porphyroblast unstrained and thus un-rotated. Others, who reacted to this study, argued that the original model was biased because of the use of Mohr Coulomb materials and a square rigid object. However further modelling using bulk coaxial strain followed by non coaxial deformation on rectangular or ovoid shapes produced the same results.

Chapter II

The above mentioned continuum mechanics possibility for the non-rotation of porphyroblasts during numerous subsequent ductile deformations, that up until the latter work was based mainly on consistent successions of changes in FIA trend and matching progressions in chemical ages, removes a major theoretical hurdle in using FIAs to resolve many problems. The FIAs measured from staurolite, andalusite and garnet porphyroblasts from an aeriially small portion of the S-shaped oroclinal Adelaide Geosyncline reveal that 5 shifts in the direction of bulk shortening, and therefore relative plate motion, took place during the Delamerian orogeny. Relative plate motion appears to have switched near orthogonally backwards and forwards twice from ~N-S dominated to ~W-E dominated in a plan view except for the last change in FIA trend. The first shift from NNW-SSE to W-E directed bulk shortening, revealed by the change from WSW-ENE trending FIA I to N-S trending FIA II, readily accounts for the S-shape of the Adelaide geosyncline. This is supported by trends in granite ages that range from 520 to 500 Ma along a WSW-ENE direction for intrusions on Kangaroo Island and Encounter Bay and 495 to 475 Ma along a N-S direction for intrusions within the N-S trending central portion of the fold belt.

Younger bulk shortening during FIAs III, IV and V reactivated or only locally refolded pre-existing structures. The correlation of the five FIA trends with peaks in the distribution of fold axial plane trends measured from geological and geophysical maps

of the Adelaide geosyncline allow the overall timing of many regional folds to be interpreted.

Chapter III

Detailed analysis of staurolite and andalusite inclusion trails in a sample containing only one FIA has revealed that the growth of both phases occurred near synchronously and very early during 3 deformation events that produced successively steep, gently dipping and finally steep axial plane structures. Neither phase reacted with the other, even where one enclosed the other. The excellent inclusion trails confirm much of and reveal more on previously described relationships on porphyroblast growth occurring early during deformation when the strain was more coaxial. They also reveal that growth ceases once the deformation becomes more non-coaxial and differentiated cleavage development commences in the proximity of a porphyroblast rim. A significant discovery was that coaxial millipede geometric effects can be present within a distinctly spiral shape.

Chapter IV

Synchronous to interleaved staurolite and andalusite growth occurred during the development of FIAs II to V which spanned ~40 million years. The Thermocalc derived pseudosections of 6 samples containing one of FIAs II, III, IV and V in both andalusite and staurolite reveal that these 2 phases are present in very similar portions of PT space. Slight differences in Mn content controlled whether garnet did or did not grow together with the other 2 phases in rocks with otherwise very similar bulk chemistries. It shifts the incoming of garnet from one side to the other of these phases on the pseudosections. This allowed the construction of tightly constrained PT paths and revealed a lengthy residency of ~40 million years for these rocks at around 3.77kb and 565°C in spite of at least 10 deformation events. This requires that from sub-vertical to sub-horizontal

foliation producing events the crust did not move up or down more than a few hundred metres. Porphyroblast growth ceased as soon as uplift began, as soon afterwards did ductile deformation.